



A Bayesian approach to understanding the key factors influencing temporal variability in stream water quality: a case study in the Great Barrier Reef catchments

Shuci Liu^{1*}, Dongryeol Ryu¹, J. Angus Webb¹, Anna Lintern^{1,2}, Danlu Guo¹, David Waters³, Andrew W. Western¹

¹Department of Infrastructure Engineering, The University of Melbourne, Parkville, VIC, 3010.

²Department of Civil Engineering, Monash University, VIC, 3800.

³Queensland Department of Natural Resources, Mines and Energy, Toowoomba, QLD, 4350.

Correspondence to: Shuci Liu (shucil@student.unimelb.edu.au)

Abstract. Stream water quality is highly variable both across space and time. Water quality monitoring programs have collected a large amount of data that provide a good basis to investigate the key drivers of spatial and temporal variability. Event-based water quality monitoring data in the Great Barrier Reef catchments in northern Australia provides an opportunity to further our understanding of water quality dynamics in sub-tropical and tropical regions. This study investigated nine water quality constituents, including sediments, nutrients and salinity, with the aim of: 1) identifying the influential environmental drivers of temporal variation in flow event concentrations; and 2) developing a modelling framework to predict the temporal variation in water quality at multiple sites simultaneously. This study used a hierarchical Bayesian model averaging framework to explore the relationship between event concentration and catchment-scale environmental variables (e.g., runoff, rainfall and groundcover conditions). Key factors affecting the temporal changes in water quality varied among constituent concentrations, as well as between catchments. Catchment rainfall and runoff affected in-stream particulate constituents, while catchment wetness and vegetation cover had more impact on dissolved nutrient concentration and salinity. In addition, in large dry catchments, antecedent catchment soil moisture and vegetation had a large influence on dissolved nutrients, which highlights the important effect of catchment hydrological connectivity on pollutant mobilisation and delivery.

1 Introduction

In-stream water quality plays a vital role in influencing the health of freshwater ecosystems (Bhaduri et al., 2016; Pérez-Gutiérrez et al., 2017), which in turn underpins environmental, social and economic sustainability (McGrane, 2016; Ustaoglu et al., 2020). Pollution derived from agricultural land and urban development has led to water quality degradation in streams and lakes in many regions of the world (Novotny, 1999; Peters and Meybeck, 2000; Ren et al., 2003; Sharpley, 2016). Among these water quality issues, coastal regions with high agricultural production have been delivering large amounts of pollutants to the ocean, where marine ecosystems are vulnerable to the evaluated levels of nutrients and sediments



(Carpenter et al., 1998; Gorman et al., 2009). It is estimated that 60% of coastal rivers in the USA have been moderately to severely degraded (Gorman et al., 2009; Howarth et al., 2002). Therefore, to protect both freshwater and marine ecosystems, better management of catchment-derived pollutants is needed.

Surface water quality is highly variable across spatial and temporal scales (Allan et al., 1997; Guo et al., 2019; Lintern et al., 2018a). These spatial and temporal variations are the result of complex interactions between three key pollutant processes in catchments, namely, sources (e.g., atmospheric deposition or anthropogenic inputs), mobilisation (e.g., detachment from the sources), and delivery (e.g., transport from sources to receiving waters) (Granger et al., 2010; Lintern et al., 2018a). Across different catchments, spatial differences in water quality concentration can vary markedly due, in part, to heterogeneity of natural landscapes in catchments (e.g., geology, topography and climate) and human-induced activities (e.g., agricultural and urban development) (Liu et al., 2018; Mainali and Chang, 2018; Mainali et al., 2019). At a site, water quality concentrations can also exhibit significant daily, event, seasonal and annual variability, driven by variations in climatic conditions, in-stream biogeochemical processes and hydrological transport (Hill, 1996; Pretty et al., 2006; Thompson et al., 2011). Thus, it can be challenging to design effective catchment water quality management strategies without a sound understanding of the spatial and temporal variation in water quality and the associated driving factors.

While it has been acknowledged that both spatial and temporal variations in water quality are of great importance for effective water resources management (Guo et al., 2020), this study focused on identifying key drivers of the temporal variability in water quality. It follows our previous study investigating spatial variation in water quality in the same region (Liu et al., 2018). A wide range of environmental factors may affect temporal changes in water quality. Runoff and rainfall have been considered as important factors and the most commonly used explanatory variables to describe temporal variation in water quality (Deletic and Maksimovic, 1998; Kim et al., 2007; Yang et al., 2009), for example early work by Hem (1948), Walling and Foster (1975) and Walling (1984). Studies considering hydrometeorological drivers have been typically related to the mobilisation and delivery of pollutants. Catchment soil moisture and evapotranspiration can also have an important role in determining the hydrological cycle (e.g., runoff generation), such as sediments (Bieger et al., 2014; Varanou et al., 2002), nutrients (Bouraoui et al., 2002; Lam et al., 2010) and salinity (Brevik et al., 2006; Tweed et al., 2007), thereby affecting the surface water quality. In addition, riverine water quality has been found to be strongly influenced by seasonal changes in vegetation cover (de Mello et al., 2018; Griffith et al., 2002; Shi et al., 2017). For instance, satellite-derived vegetation indices have provided an opportunity to explore the relationship between land cover and water quality temporal dynamics (Fu and Burgher, 2015; Griffith, 2002; Singh et al., 2013; Whistler, 1996). Even though significant research efforts have been made to explore the relationship between water quality and these environmental conditions, a comprehensive understanding of their relative importance in diverse environments and at large scales is still lacking.

Statistical modelling has been widely used to investigate water quality temporal dynamics in response to changes in the abovementioned environmental factors (Alexander et al., 2002; Fu et al., 2019; Miller et al., 2014; Singh et al., 2013; Zhang and Blomquist, 2018; Zhang et al., 2016; Zhang and Schilling, 2005). However, existing studies have limitations. Firstly,



65 water quality monitoring data have often been limited to low sampling frequencies, typically using monthly grab samples. This can result in a lack of information on water quality dynamics over runoff/storm events, which is when a significant proportion of nutrients and sediment loads are transported (Lloyd et al., 2016; Sherriff et al., 2015). Secondly, most studies on statistical water quality modelling have only investigated the relationship between water quality and explanatory variables in a single or limited number of catchments in small regions (Chang et al., 2015; Khan et al., 2020; Koci et al., 2020; Liu et al., 2008b; Noori et al., 2020; Wang et al., 2016; Zhang et al., 2016). Few studies have investigated water quality at multiple locations using the same modelling framework. Lastly, studies have usually relied on a single ‘best’ model with an assumption that it best approximated the true drivers of water quality (Paliwal et al., 2007; Zhang et al., 2009). This ignores the issue of selection uncertainty. Furthermore, relying on a single model structure might result in misleading conclusions or overconfidence in the results (Link and Barker, 2006; Wintle et al., 2003).

75 This study attempted to address these knowledge gaps, taking advantages of event-based water quality monitoring data from the Great Barrier Reef (GBR) catchments in northern Australia, where land-derived pollutants have posed threats to ecosystem of the GBR lagoon (Brodie et al., 2012; Hunter and Walton, 2008; McKergow et al., 2005b; Waterhouse et al., 2017). We targeted nine common water quality indicators, including sediments, nutrients and salinity. Bayesian hierarchical modelling was used to investigate water quality spatial and temporal variation. This allowed the prediction of water quality in multiple catchments, as well as simultaneously quantifying parameter uncertainty (Gelman et al., 2013; Rode et al., 2010; Webb and King, 2009). In addition, we used Bayesian model averaging (BMA) approaches to identify the relative importance of the different environmental factors and provide multi-model weighted predictions, which have been shown to better quantify the uncertainty arising from model selection (Höge et al., 2019; Raftery et al., 1997; Wang et al., 2012). Overall, this study aimed to: (1) identify the key drivers of temporal variation in water quality; and (2) predict water quality temporal variation using a Bayesian multi-model approach.

85

2 Materials and methods

2.1 Study area

The GBR catchments, situated in north-eastern Australia (Figure 1), consist of six natural resource management regions whose streams and rivers discharge into the Great Barrier Reef lagoon. These catchments cover a 437,354 km², approximately a quarter of the state of Queensland, and exhibit significant diversity in climatic, geological and topographical landscape characteristics, as well as in land use and land management (Bartley et al., 2018; Gilbert and Brodie, 2001). The GBR catchments range from small, steep, high-energy streams in the wet tropics, which are dominated by sugarcane crops and rainforest, to large inland catchments used for savannah grazing, and crops (e.g., grain) and with extensive low energy floodplains in the dry tropics (Table 1) (Davis et al., 2017; Koci et al., 2019; McKergow et al., 2005a). Spatial and temporal variations in rainfall in the GBR catchments are a major cause of the diversity in land use patterns. Annual rainfall ranges from less than 500 mm in the south-west to more than 8000 mm in the north-east (Figure 2 [c]) (Davis et al., 2017; Kuhnert

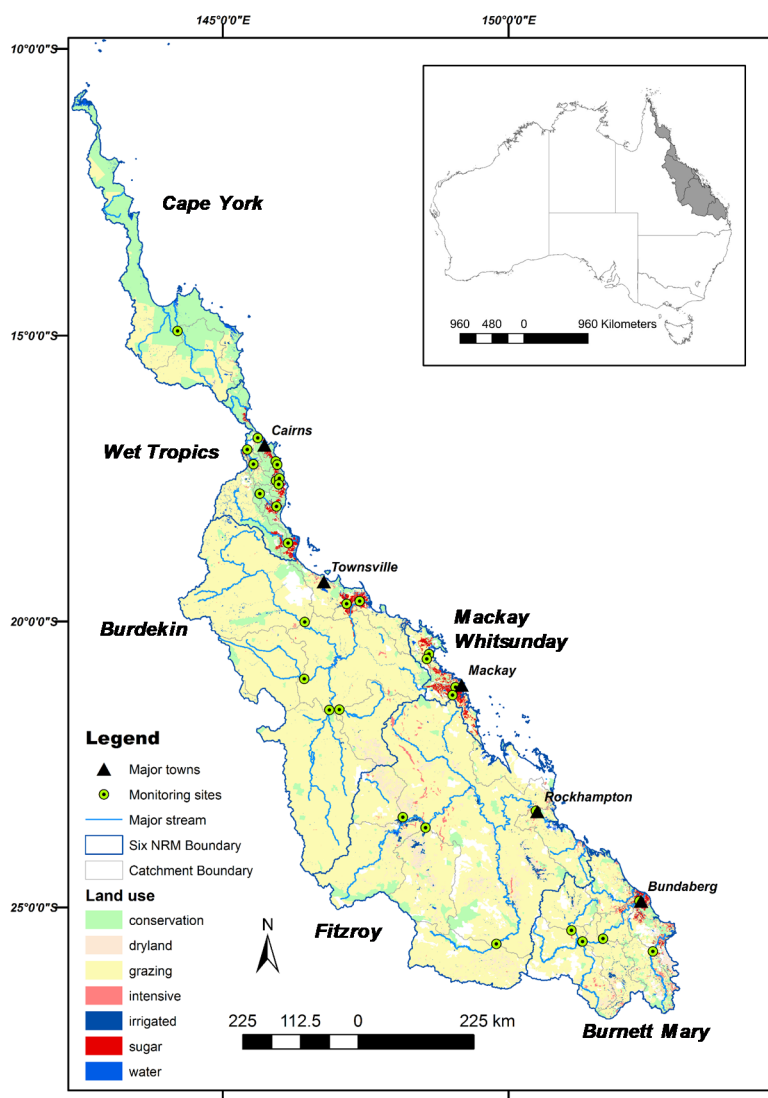
90

95



et al., 2009). Distinct wet (November to April) and dry (May to October) seasons result in high seasonal variation in runoff and El Nino-Southern Oscillation (ENSO) leads to high inter-annual variability (Day and McKeon, 2018; Murphy and Ribbe, 2004). In the dry tropics, a few large events in the wet season contribute the majority of annual runoff, and constant low flow dominates during the dry season (Jarihani et al., 2017).

Thirty-two sites within the GBR catchments were selected as case study catchments (Figure 1 and Table C1 in Appendix C). Previous multivariate analysis of the patterns of time-averaged concentrations indicated that there were two groups of sites (Table 1 and Figure 2 [a]), which was a result of spatial heterogeneity in catchment landscape characteristics (Figure 2 [b], [c] and [d]) (Liu et al., 2018).



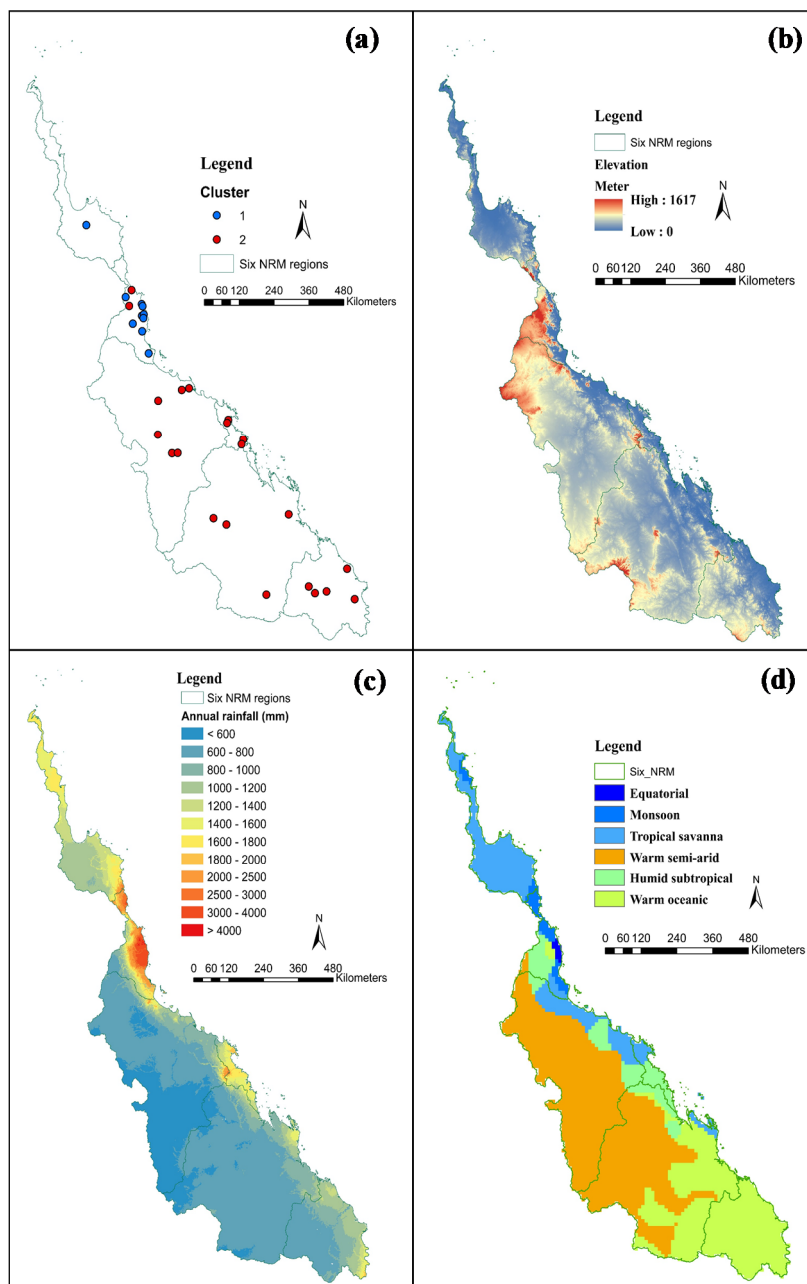
105

Figure 1. The Great Barrier Reef catchments, monitoring sites, land uses and the six natural resource management (NRM) regions. Land uses have the following characteristics: (1) conservation (forest, woodland, savannah, etc for conservation



110

purposes); (2) dryland (rainfed agriculture including cereals but excluding grazing and sugar cane); (3) grazing (primarily cattle grazing of native and introduced vegetation); (4) intensive (urban areas, roads, etc); (5) irrigated (irrigated cropping excluding sugar cane); (6) sugar (rain-fed and irrigated sugar cane); and (7) water (water bodies, including lake, river, and marsh/wetland).



115

Figure 2: Spatial information of the GBR catchments in northeast of Australia: [a] site locations showing two groups based on clustering analysis of spatial variability in time-averaged water quality (Liu et al., 2018); [b] topographic elevation (250 m resolution) (Geoscience Australia, 2008); [c] annual average rainfall (Bureau of Meteorology, 2012), and [d] updated Köppen-Geiger climate zone classification (Peel et al., 2007).



Table 1: Summary of differences in landscape characteristics between the two clusters of sites (Liu et al., 2018).

Cluster	Climate	Hydrology	Land use/land cover	Topography
1	Wet tropics region with high annual rainfall	Perennial, high energy rivers	Dominated by conservation (e.g. rainforest), and cropping (e.g. sugar)	Small and steep
2	Mostly dry tropics, relatively dry with clear seasonal variability in rainfall	Ephemeral, low energy rivers, cease-to-flow in dry period	Dominated by brigalow native vegetation, and pastures for grazing,	Large and flat

2.2 Data collection and preparation

2.2.1 Water quality data

The nine studied constituents were total suspended solids (TSS), particulate nitrogen (PN), oxidized nitrogen (NO_x), ammonium nitrogen (NH₄), dissolved organic nitrogen (DON), filterable reactive phosphorus (FRP), dissolved organic phosphorus (DOP), particulate phosphorus (PP), and electrical conductivity (EC). Water quality monitoring data collected for the 32 GBR catchments over the 11-year period of 2006 to 2016 were obtained from the Loads Monitoring Program (Turner et al., 2012). This dataset contained both high-frequency event-based samples (e.g., daily or every few hours by automatic samplers) that were taken during runoff events, as well as grab samples (e.g., monthly) that were taken under baseflow conditions (Orr et al., 2014; Waters et al., 2013; Waters and Packett, 2007). As EC data from the Loads Monitoring Program were limited, we extracted additional EC data from the Water Monitoring Information Portal provided by the Department of Natural Resources, Mines and Energy of Queensland (DNRME, 2018) to complement the Loads Monitoring Program records.

2.2.2 Event mean concentration

We extracted continuous discharge records for each site from the Water Monitoring Information Portal (DNRME, 2018) to identify individual runoff events. An automated hydrograph analysis tool – *HydRun* (Tang and Carey, 2017) was used to delineate runoff events. The start and end points of a specific event were determined by using a local-minimum method that calculates the first derivative of the streamflow record (separated from baseflow). The event-mean concentration (EMC) was then calculated for each event that had at least two samples on each of the rising and falling limbs of the hydrograph. This ensured that the water quality dynamics over a runoff event were reasonably well-captured, and that the derived EMCs were reliable (Waters and Packett, 2007). For each event, the EMC of a constituent was calculated as the total load per unit flow volume within the event using (Bartley et al., 2012; Joo et al., 2012):



$$EMC = \frac{EventLoad}{EventFlowVolume} = \frac{\sum_{j=0}^n \frac{c_j + c_{j+1}}{2} \times q_{j+1/2} \times t_{j+1/2}}{\sum_{j=0}^n q_{j+1/2} \times t_{j+1/2}} \quad (1)$$

where n is the total number of samples for a given event, c_j is concentration of the j^{th} sample, $q_{j+1/2}$ and $t_{j+1/2}$ are the inter-sample mean discharge and time interval between j^{th} and $(j+1)^{th}$ samples. The concentrations at the start and end of the event (c_0 and c_{n+1}) are assumed to be the averaged value for samples during baseflow (with baseflow identified in the previous section). The EMCs were essentially flow-weighted mean concentrations over individual runoff events, which allowed the comparison of water quality across catchments with contrasting flow regimes (e.g., two clusters of sites in Figure 2) (Cooke et al., 2000; Richards and Baker, 1993). A total of 1412 events was identified across the 32 sites, and, depending on data availability, EMCs were calculated for between 21% (DOP) and 43% (TSS) of these identified runoff events (Table C2).

The derived EMCs were Box-Cox transformed to improve the symmetry of the response variable (Box and Cox, 1964) to improve model fitting (Hawkins and Weisberg, 2017; Lawrance, 1988; Zhang and Yang, 2017). The site-level Box-Cox transformation parameter λ for each constituent was first identified, using the *car* package in *R* (Fox et al., 2012; R Core Team, 2013). Then, for each constituent, the average λ from the 32 sites was used to transform all available EMCs for that specific constituent. This ensured that an identical transformation parameter was applied across the different sites for each constituent (Guo et al., 2019).

2.2.3 Explanatory variables

This study investigated the effect of various hydrologic, climatic and vegetation cover characteristics for different events. These characteristics included runoff, catchment root zone soil moisture, actual evapotranspiration rainfall, air temperature, and vegetation cover. The continuous streamflow monitoring data, gridded weather and climatic products, and remotely sensed imagery were used to derive catchment average conditions for each event (Table 2).

Table 2. Explanatory variables and their data sources

Explanatory variable	Unit	Spatial resolution	Source
Daily runoff	mm/d	point measurements	Queensland Department of Natural Resources, Mines and Energy (DNRME, 2018). Available from https://water-monitoring.information.qld.gov.au/
Daily rainfall	mm	5 km × 5 km	Australia Water Availability Project (AWAP) (Raupach et al., 2009). Available from http://www.csiro.au/awap/
Daily temperature	°C		
16-day normalized difference vegetation index (NDVI)	-	1 km × 1 km	Moderate Resolution Imaging Spectroradiometer (MODIS) - MOD13A2v006 (Didan, 2015). Available from https://earthdata.nasa.gov/
Daily soil moisture (root zone 0 -100 cm)	mm	5 km × 5 km	Australia Landscape Water Balance model (AWRA-L) (Frost et al., 2016). Available from http://www.bom.gov.au/water/landscape
Daily actual ET	Mm		



Note: ET – evapotranspiration

For individual runoff events identified in the previous section, three groups of event characteristics were prepared, characterising pre-event, during-event and post-event conditions (Table 3). Except for runoff, data for all explanatory variables were first extracted from gridded data using catchment boundaries were delineated using the Geofabric tool provided by the Australian Bureau of Meteorology (Bureau of Meteorology, 2012) (Figure 1). The catchment average time series data were then averaged over the specific time-window related to the event (Table 3).

Table 3: Three groups of event characteristics and averaging method

Group	Explanatory variable	Abbreviation used in figures and tables in paper	Calculation method
During-event	Average runoff	Event_ave_Q	Average of daily runoff during event
	Maximum runoff	Event_max_Q	Maximum of daily runoff during event
	Average rainfall	Event_ave_P	Average of daily rainfall during event
	Maximum rainfall	Event_max_P	Maximum of daily rainfall during event
	Average temperature	Event_T	Average of daily temperature during event
	Average NDVI	Event_NDVI	Average of NDVI during event
	Average soil moisture	Event_SM	Average of daily soil moisture during event
	Average actual ET	Event_AET	Average of daily actual ET during event
Pre-event	Average runoff	Ante_Q	Average of daily runoff for 7 days prior to event
	Average rainfall	Ante_P	Average of daily rainfall for 7 days prior to event
	Average NDVI	Ante_NDVI	Average of NDVI for 3 months prior to event
	Average soil moisture	Ante_SM	Average of daily soil moisture for 7 days prior to event
	Average actual ET	Ante_AET	Average of actual ET for 7 days prior to event
Post-event	Average runoff	Post_Q	Average of daily runoff for 7 days after event

Note: Q – runoff; P – rainfall; T – temperature; NDVI – normalized difference vegetation index; SM – root zone soil moisture; ET – evapotranspiration.

The explanatory variables in the during-event conditions were averaged over the duration of the event. For the pre-event and post-event conditions, the 7 days prior to and after the event were used as the time-window (except NDVI). The 7-day period was the median of the time of concentration (i.e., the time for runoff to travel from the most remote point of the catchment to the monitoring site) across all catchments. These were estimated from catchment topography using the Bransby-William's equation, following its wide application in Australian catchments for flood estimation (French et al., 1974; Pilgrim et al., 1987). The ground cover was quantified by NDVI, an indicator of the biophysical condition of the vegetation canopy (Griffith et al., 2002). Previous studies have also shown that there is a time-lag between water availability and a change in ground cover, which is typically three months for Australian catchments (De Keersmaecker et al., 2015; Papagiannopoulou et al., 2017). Therefore, to represent the pre-event ground cover condition, we averaged all available NDVI measurements

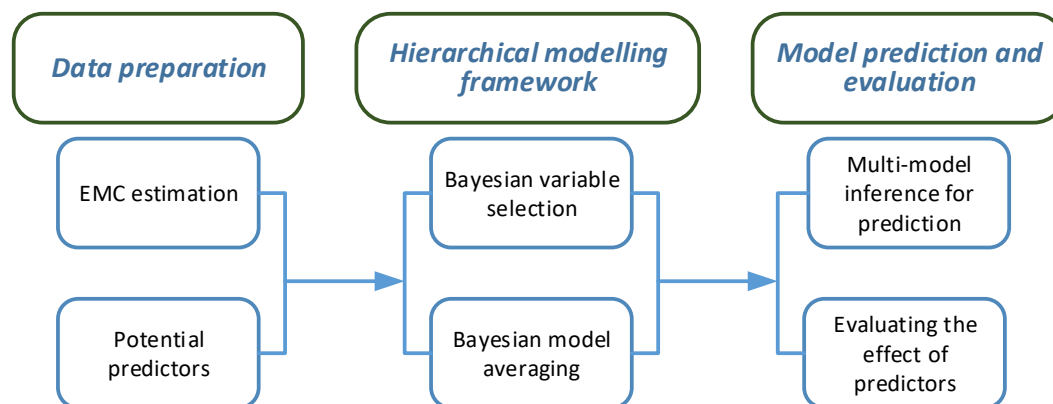


for three months prior to an event. The runoff after the event (7 days) was also included as an indicator of catchment wetness at the end of the event, to assess if hydrologic condition towards the end of an event influences the temporal variation in water quality.

180 Similar to the EMCs, all the explanatory variables were Box-Cox transformed following the procedure described in Sect. 2.2.2. In addition, prior to the analyses, both transformed EMCs and explanatory variables were standardized to a mean of zero and standard deviation of one. As such, the magnitude of a coefficient indicates the effect of each predictor relative to other predictors (Wan et al., 2014). The cross-correlation (non-parametric Spearman’s Rank correlation coefficient) of all transformed predictors is provided in Figure B1, Appendix B.

185 2.3 Modelling: driver identification and water quality prediction using multi-model inference

The statistical analysis and modelling followed several steps (Figure 3). The Bayesian modelling framework was applied to catchments in Clusters 1 and 2 separately. This is because we assumed that the key drivers of temporal variability in water quality would differ between two Clusters due to their differences in land use and climate.



190

Figure 3: Analyses steps; the detailed methods used in the hierarchical modelling framework and model prediction and evaluation are in the following sections.

2.3.1 Bayesian variable selection

To investigate the relative importance of individual predictors, an indicator Bayesian variable selection method was used called Gibbs variable selection (GVS) (George and McCulloch, 1993; Ntzoufras, 2002). An auxiliary inclusion variable I_n (Eq. (2)) for each predictor was introduced to indicate whether that predictor was ‘in’ or ‘out’ of an individual iteration of the hierarchical modelling structure.

$$I_n \begin{cases} 1, & n^{th} \text{ predictor present} \\ 0, & n^{th} \text{ predictor absent} \end{cases} \quad (2)$$



I_n was modelled at the top level of the hierarchy which enabled the use of identical model structures (i.e., combination of predictors) across different sites. The overarching hierarchical modelling framework was defined as follows:

$$y_{i,j} \sim N(\mu_{i,j}, \sigma) \quad (3)$$

$$\mu_{i,j} = \overline{mean}_j + \overline{std}_j \times \Delta_{i,j} \quad (4)$$

$$\Delta_{i,j} = \sum_{n=1}^N \theta_{n,j} \times x_{n,i,j} \quad (5)$$

$$\theta_{n,j} = I_n \times \beta_{n,j} \quad (6)$$

200 The data-level model (Eq. (3)) assumed that the EMC of a particular constituent (e.g., one of TSS, NO_x, EC, etc) at i^{th} time step in the j^{th} sub-catchment, $y_{i,j}$, followed a normal distribution (denoted as $N(\cdot)$), with mean $\mu_{i,j}$ and a global standard deviation σ . The mean value, $\mu_{i,j}$ was modelled as the observed site-level averaged EMC \overline{mean}_j plus $\overline{std}_j \times \Delta_{i,j}$, with the latter term being defined as the deviation from this averaged value (Eq. (4)) (Guo et al., 2019). The deviation term incorporated the site-level observed standard deviation \overline{std}_j , making $\Delta_{i,j}$ a standardised measure that could be compared

205 across sites. $\Delta_{i,j}$ was further modelled as a linear additive function (Eq. (5)) of all candidate predictors x_n in $n = 1, 2, \dots, N = 14$ (e.g., event average runoff, rainfall and NDVI). Consequently, $\Delta_{i,j}$ was defined as the temporal variability in water quality, and was the quantity of interest. The effect size ($\theta_{n,j}$) of individual predictors was another latent variable used in the GVS, and was estimated as the product of I_n and the regression coefficient $\beta_{n,j}$ (Eq. (6)), such that $\theta_{n,j}$ was either $\beta_{n,j}$ ($I_n = 1$), or 0 ($I_n = 0$).

210 2.3.2 Hierarchical prior specification and Bayesian inference of key drivers

Bayesian inference required specification of prior distributions for each model parameter. We used a hierarchical conditional prior specification for predictor coefficients, allowing the site-specific parameter values that describe the effects of each of the temporal predictors ($\beta_{1,j}, \beta_{2,j}, \dots, \beta_{n,j}$) to be exchangeable between sites (Liu et al., 2008a; O'Hara and Sillanpää, 2009; Webb and King, 2009). The detail specification of priors for each model parameter can be found in Appendix A. In addition,

215 to identify key drivers affecting temporal changes in water quality, the posterior inclusion probability (PIP - $P(I_n = 1|y)$, Eq. (A8) in Appendix A) of each predictor was used to compare the relative importance of individual predictors (i.e., how often the n^{th} predictor was 'in' the model).

2.3.3 Prediction from multi-model inference

We used Bayesian Model Averaging to generate an ensemble of predictions of temporal variation in EMC for individual

220 constituents (Eq. (7)). The average posterior distribution of a quantity of interest (i.e., temporal variability in EMC) was



generated using the parameters (e.g., $\beta_{1,j}$, $\beta_{2,j}$, ..., $\beta_{n,j}$) sampled from the posterior distribution to simulate EMC values using the specific model, defined as follows:

$$[\hat{y}|y] = \sum_{x=1}^L [\hat{y}|y, M_x] P(M_x|y) \quad (7)$$

where $[\hat{y}|y, M_x]$ is the posterior distribution of a vector \hat{y} of (prediction) derived from model M_x , and $P(M_k|y)$ is the
225 posterior model probability (PMP, Eq. (A8), in Appendix A) (Hooten and Hobbs, 2015; O'Hara and Sillanpää, 2009).

2.3.4 Model evaluation and implementation

The proposed modelling framework was applied to the two clusters of sites independently. This allowed an investigation of whether the spatial heterogeneity in catchment landscapes led to differences in the key factors controlling temporal variation in water quality. The key drivers were determined as the predictors with a PIP above 0.8 (i.e., over 80% of the models
230 included these predictors).

To further understand the reliability and robustness of the BMA framework, the consistency of the posterior inclusion probability of individual predictors was investigated by resampling subsets of the observations multiple times (Kohavi, 1995). For each cluster, 80% of events within one site were first randomly selected and the posterior inclusion probability for this subset of observations was estimated. This was repeated 1,000 times to produce a distribution of posterior inclusion
235 probabilities for individual predictors, which was then used to assess the uncertainty in the posterior inclusion probability.

An ensemble of the averaged prediction in temporal variability of each event was obtained from each iteration of parameter updating using Markov chain Monte Carlo (MCMC). The model fit was evaluated using the Nash-Sutcliffe coefficient (NSE) (Nash and Sutcliffe, 1970) between the observed temporal variability and the median of ensemble predictions \hat{y} derived from the BMA (Eq. (7)). The NSE was calculated at both the cluster- and site-levels. The model residuals were also
240 checked for normality and heteroscedasticity (i.e., relationship between the residual and predictors). In addition, model performance was evaluated by providing the 50% and 95% credible interval (CI) of each prediction.

To compare the relative importance of the predictors that have been widely used in existing literature (i.e., runoff and rainfall) and other predictors (e.g., soil moisture, temperature, evapotranspiration, and vegetation cover), the modelling framework was re-calibrated using only the rainfall/runoff related predictors (including all pre-, during- and post-event
245 predictors). This estimated the degree of improvement in the model's explanatory power with the inclusion of environmental variables, such as catchment wetness and ground vegetation cover conditions.

The hierarchical modelling framework was implemented in *JAGS* (Plummer, 2003, 2013a), using the package *rjags* in *R* (Plummer, 2013b; R Core Team, 2013), which enabled both the estimation of parameter values from prior distributions with Markov chain Monte Carlo (MCMC) and the generation of model-averaged predictions. The MCMC sampling had three
250 parallel chains with 25,000 iterations for each chain. The first 5,000 iterations were discarded as a 'burn-in' period to allow



convergence of the Markov chains, resulting in 60,000 values to estimate the posterior distribution for each model parameter and make model predictions.

3. Results

3.1 Key drivers of temporal variability in water quality

- 255 The three key measures that were used to quantify the effect of individual predictors are: (1) estimates of posterior inclusion probability (PIP), which quantifies relative importance of individual predictors; (2) posterior model probability (PMP), which estimates differences in plausible model structures; and (3) posterior distributions of coefficients for the key drivers (i.e., effect size, e.g., $\theta_{1,j}$, $\theta_{2,j}, \dots, \theta_{n,j}$ in Eq. (6)), which measures direction and magnitude of the effect of key predictors on water quality temporal variability.
- 260 Posterior inclusion probability (Figure 4 and Table C3 in Appendix C) from the Bayesian modelling results indicated that, in general, antecedent vegetation condition and antecedent soil moisture were key factors in explaining temporal variation in water quality, especially for Cluster 2 (warmer, drier) sites. Catchment runoff and rainfall were the second most important group of factors, especially for particulate pollutants (TSS, PN and PP; Clusters 1 and 2) and salinity. In addition, the three groups of predictors (pre-, during-, post-event) showed varying effects among the constituents. With regard to during-event
- 265 conditions, event average runoff (*Event_ave_Q*), event maximum runoff (*Event_max_Q*) and event average rainfall (*Event_ave_P*) were three important factors with relatively high PIP. In contrast, among pre-event conditions, antecedent NDVI (*Ante_NDVI*) and antecedent soil moisture (*Ante_SM*) were driving factors for the majority of the constituents. Post-event runoff (*Post_Q*) only affected a few constituents (e.g., on NO_x and FRP for Cluster 2), compared with the other two groups of predictors. Overall, there were notable differences in the important predictors for Clusters 1 and 2, and more
- 270 important predictors were found for the Cluster 2 sites.

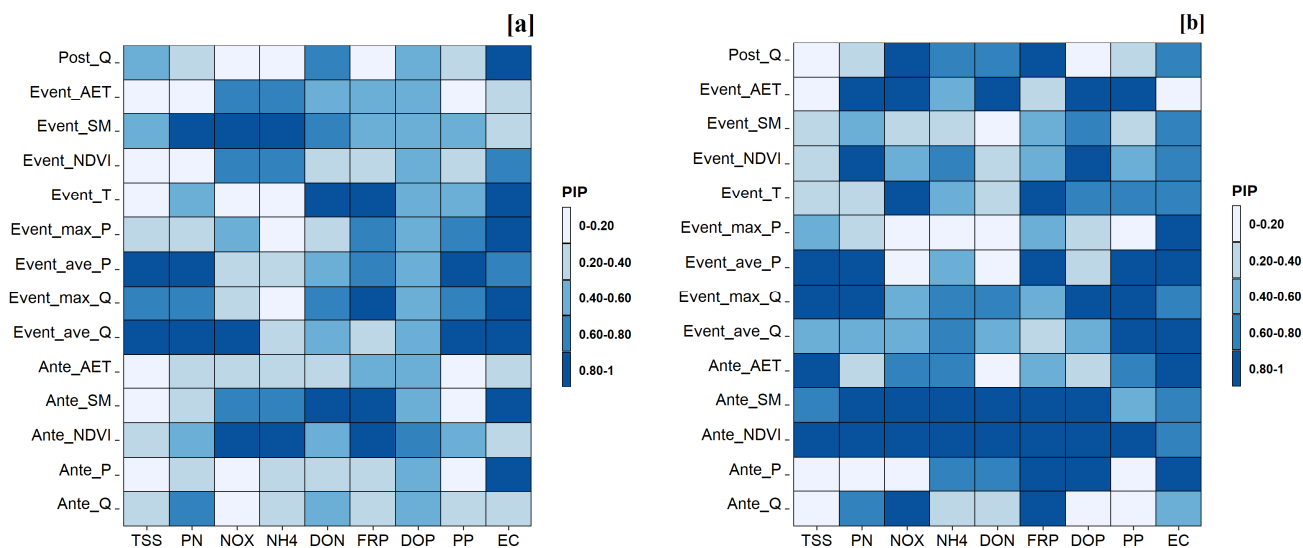
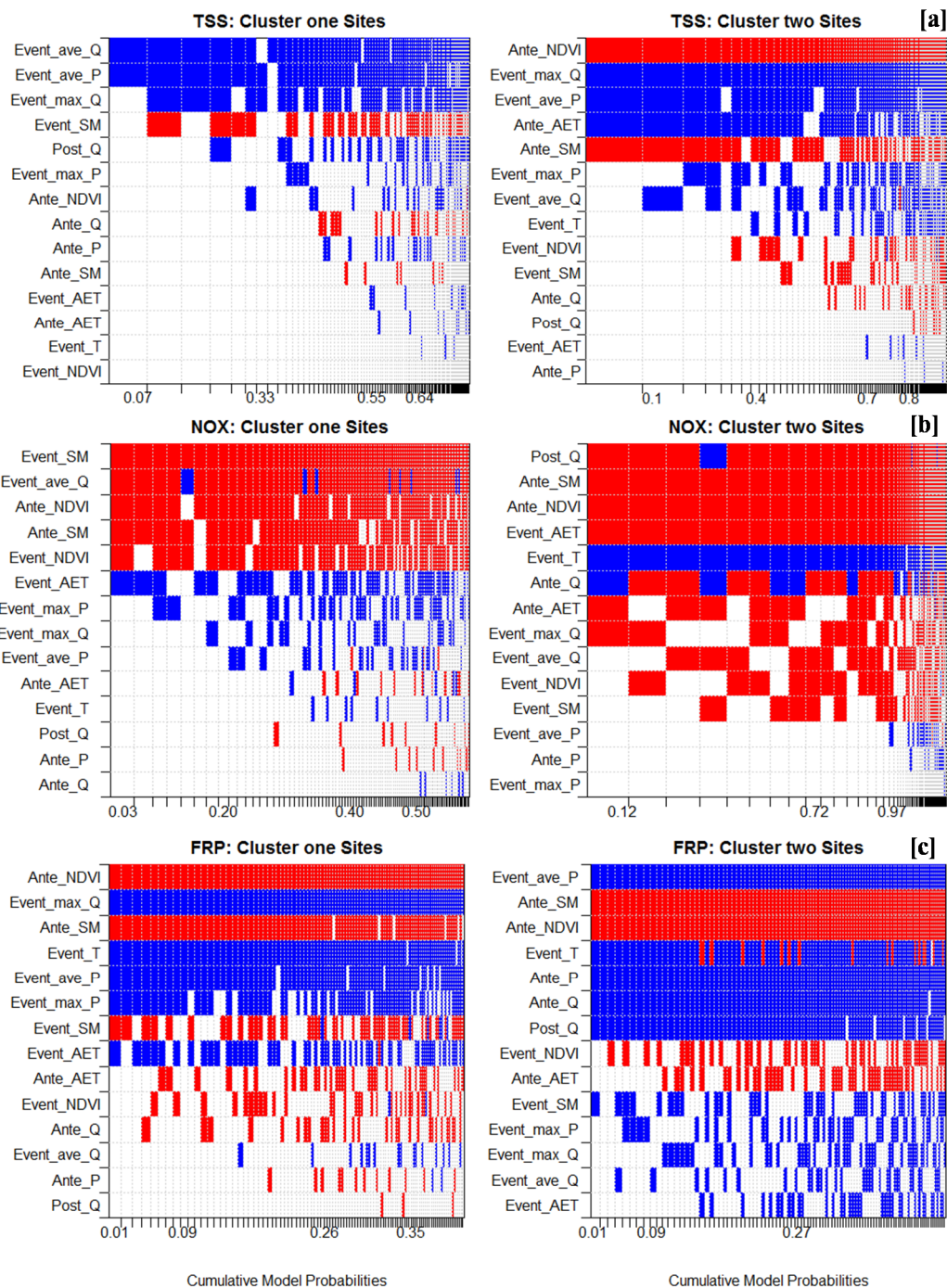


Figure 4: Posterior inclusion probability (PIP) of each candidate predictor for [a] Cluster 1 (“wet”) catchments, and [b] Cluster 2 (“dry”) catchments; dark blue = high PIP; light blue = low PIP. The definition of the abbreviations of each predictor on the y-axis are in Table 3.

275

Results from here on will focus mainly on TSS, NO_x and FRP, due to their impacts on the marine receiving environment. Results for the other six constituents are in the Supplementary Materials. Figure 5 shows the posterior model probabilities for TSS, NO_x and FRP for the 100 models with highest PMP (Figures B2 and B3 in Appendix B show other constituents). Red indicates a negative influence and blue a positive influence. The difference in PIP between the two clusters resulted in quite different plausible model structures (models with relatively high posterior model probability). A stand-out difference between the results for the two Clusters was antecedent vegetation cover condition (*Ante_NDVI*), which tended to be a more important predictor of TSS for Cluster two, than for Cluster one (Figure 5 [a]). In addition, the plausible models for Cluster 2 were generally more complex (with a larger number of predictors), except for DOP and EC (Figures B2 and B3).

280



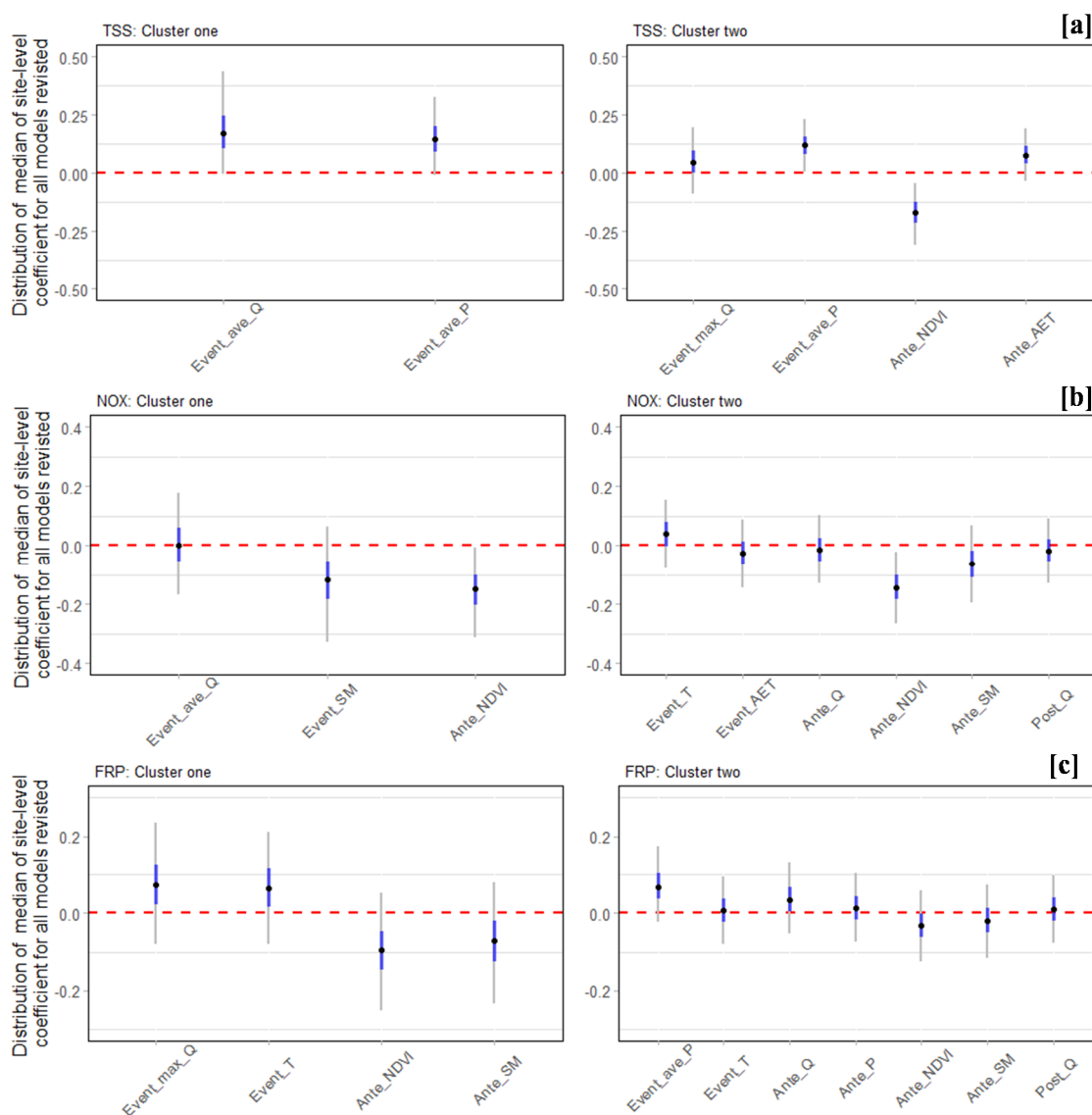
285

Figure 5: Comparison of BMA model coefficients and cumulative model probabilities (only the first 100 models ranked according to the highest probability are shown) between Cluster 1 (“wet” - left) and Cluster 2 (“dry” - right) sites for [a] TSS, [b] NO_x and [c] FRP. The order of predictors on the y-axis was ranked based on the posterior inclusion probability. Each column in the heatmap represents the one specific model (ranked from highest model probability from left to right) and the width of the column



290 is normalised by the posterior model probability (i.e., the widest columns indicate models with the largest increase in probability compared to the next most probable model). The colour indicates the direction of the coefficients: red = negative; blue = positive. The coefficient value was averaged across the posterior median value of the site-specific coefficient within each cluster (effect size, $\theta_{n,j}$, in Equation 6); the definition of the abbreviations of each predictor on the y-axis are in Table 3.

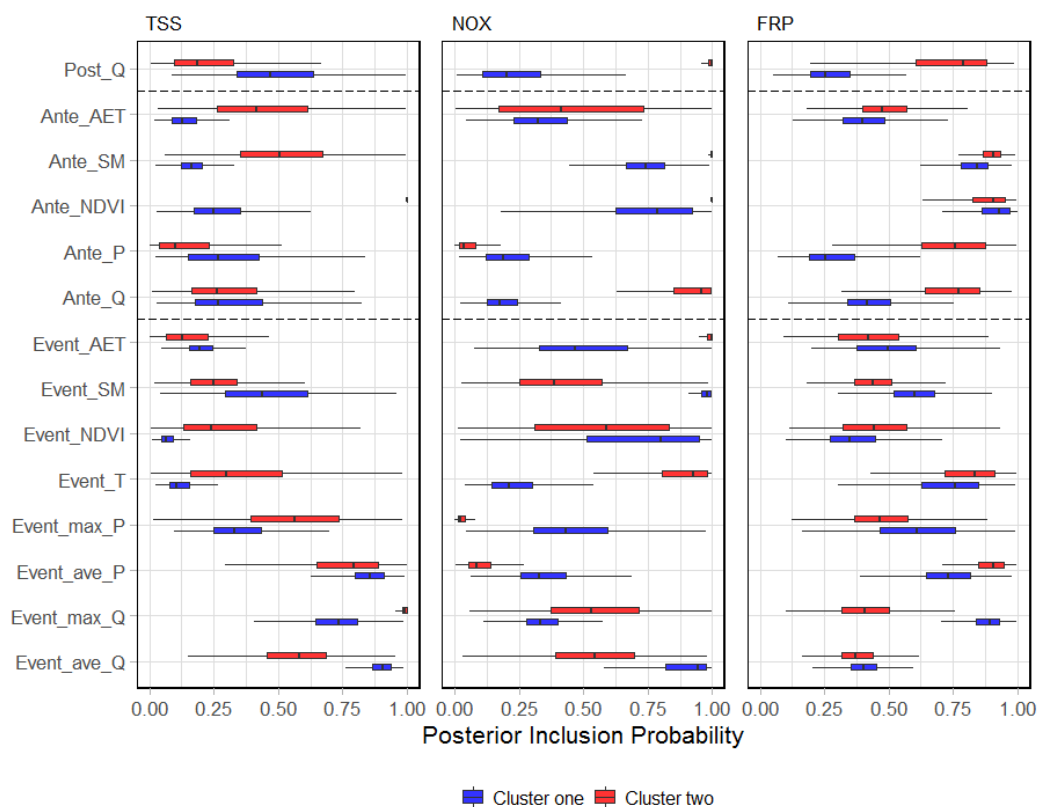
295 The distribution of posterior model coefficients for the key predictors (Figure 6, Figures B4 and B5) further demonstrated that the key drivers of temporal variability in water quality vary between catchments and between constituents. During-event runoff and rainfall tended to have a positive effect on sediment and particulate constituents and, a negative effect on NO_x and EC. In addition, there was strong negative effect of antecedent vegetation condition on the majority of the constituents.





300 **Figure 6: Distribution of median of site-level coefficients for all plausible models in BMA between Cluster 1 (“wet” - left) and**
Cluster 2 (“dry” - right) sites for: [a] TSS; [b] NO_x and [c] FRP. Only predictors with PIP > 0.8 are included. For each specific
model structure, the coefficient value of a predictor was the median of the site-specific coefficient across all sites (effect size, $\theta_{n,j}$, in
Eq. (6)). The distribution of this value thus represents the probability of the model (PMP), as well as variability in the same
 305 **predictor across different sites; black dots = the median; grey vertical lines = 95% CI; blue coloured vertical lines = 50% CI; the**
definition of the abbreviation of each predictor on x-axis are in Table 3.

The uncertainty in PIP, derived from 1,000 subsampled BMA runs (Figure 7, Figures B6 and B7) highlighted that the BMA
 results were robust for most constituents, except for EC (Figure B7 [c]). BMA tends to identify important predictors and less
 sensitive to the input data which is evidenced by the relatively narrow range of interquartile ranges (IQR), when PIP for a
 specific predictors is large (e.g., antecedent soil moisture for FRP in Figure 7). It is also worth noting that large uncertainty
 310 in the PIP for EC was observed, indicating the BMA results were sensitive to the observations of EC. This might be related
 to data availability, which is further discussed in Sect. 4.2.

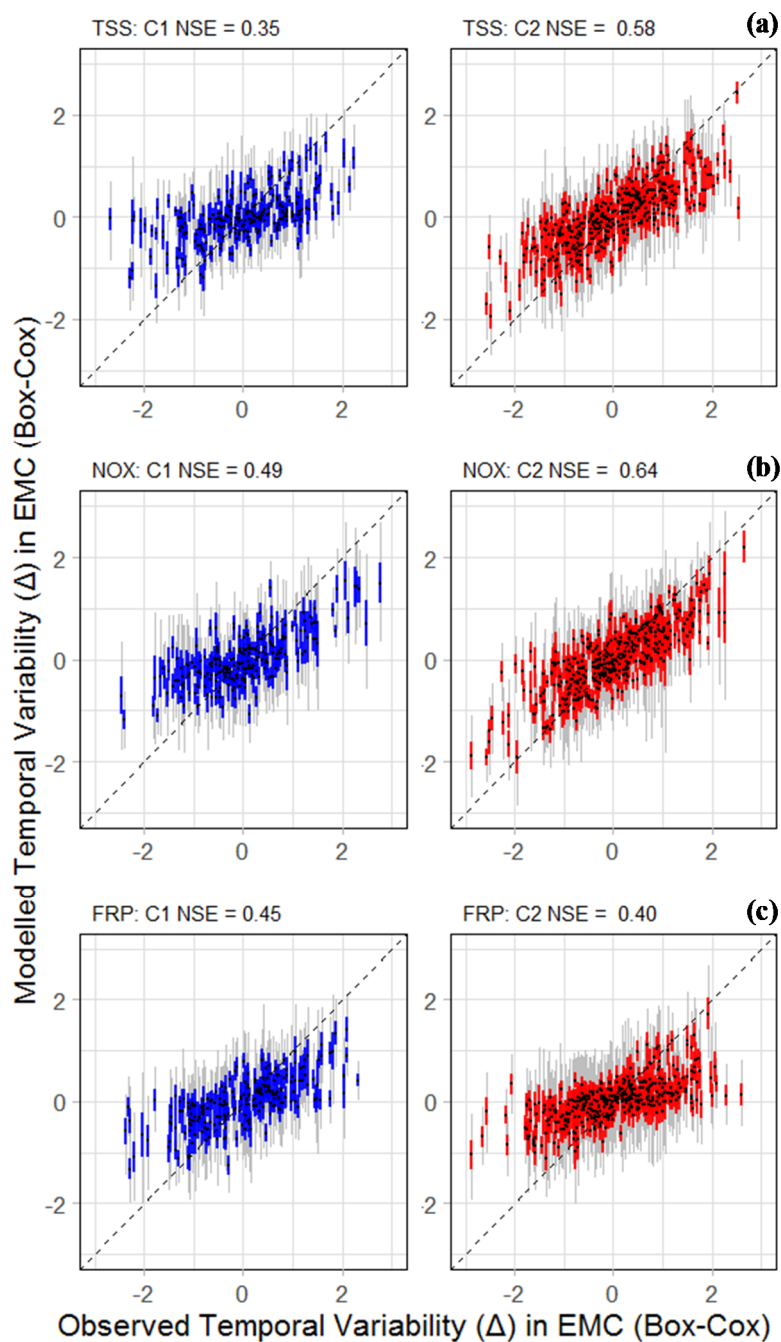


315 **Figure 7: The comparisons of the distribution of posterior inclusion probabilities of the individual predictors derived from 1,000**
subsampled BMA runs; the boxes are the interquartile ranges (IQR, 25th to 75th percentile), and the whiskers are the ranges
between 1.5 IQR of the lower quartile and 1.5 IQR of the higher quartile; the vertical bar = median; blue = Cluster 1 (“wet”); red
= Cluster 2 (“dry”); the definition of abbreviation of each predictor on y-axis are in Table 3.



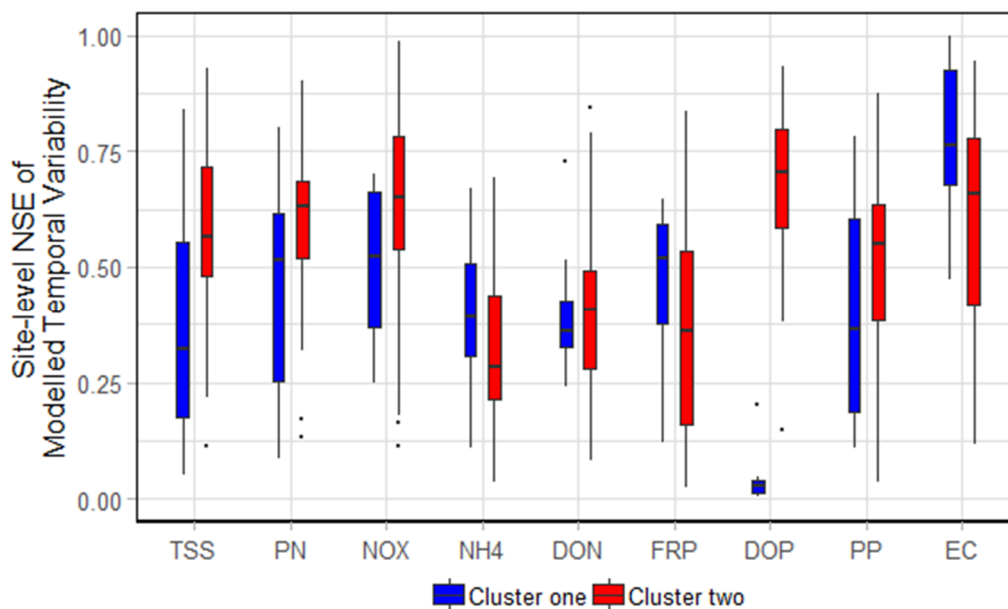
3.2 Predictive performance

Moderate levels of temporal variability were explained by the BMA framework for the two independent clusters of sites (Figure 8, Figures B8 and B9). At the cluster level, the NSE ranged from 0.04 (DOP) to 0.68 (EC) and from 0.34 (NH₄) to 0.64 (NO_x) for Clusters 1 and 2 (full model columns in Table 4), respectively. The comparison of the modelling performance (posterior median of BMA prediction) showed that the modelling framework performed better on the Cluster 2 sites than Cluster 1 (Figure 8, red 50% prediction CI – Cluster 2), except for NH₄ and EC (not shown). This was reflected in a better match to the 1:1 line within the 90% prediction CI for Cluster two catchments. It is also worth noting that the prediction interval for EC (Figure B9 [c]) was much wider than the rest of the constituents. Similar results were found in the site-level performance, with the average site-level NSE (Figure 9) for Cluster 2 models typical higher than for Cluster 1. The site-specific performance varied across sites, with the largest variation in EC (NSE for the Cluster 2 result ranged from approximately 0.20 to 0.90). The modelling performance of DOP in the Cluster 1 sites was poor (NSE = 0.04); all candidate covariates had low predictive power, resulting in the poor mixing of chains of the inclusion variable I_n (i.e., posterior I_n was around 0.5). The model residuals were normally distributed (Figure B10) and there was no clear heteroscedasticity within the residuals (Figures B11 to B19).



335

Figure 8: Performance of the BMA models of the temporal variability of three constituents across 32 sites, represented by prediction intervals from BMA and observed Box-Cox EMC across two clusters of sites for: (a) TSS; (b) NO_x; and (c) FRP. Each bar shows a single event and all events at all sites in the cluster are included. The NSE values were calculated based on median predictions. Black dots show prediction median; grey vertical lines show 95% CI; coloured vertical lines show 50% CI; blue is Cluster 1 (“wet”); red is Cluster 2 (“dry”); and dashed black lines are the 1:1 relationship.



340 **Figure 9: Distribution of site-level NSE for modelled the temporal variability of two clusters of sites. The interpretation of boxplot is the same as Figure 7. NSE values were calculated based on site-level predictions of event median EMC; blue is Cluster 1 (“wet”); and red is Cluster 2 (“dry”) (i.e., each boxplot is comprised of respective number of sites in each cluster, one for each catchment).**

Table 4 compares the model performance using rainfall/runoff related predictors only and all candidate predictors (full model). A large increase in NSE was found for most dissolved nutrient species (e.g., NO_x, NH₄, DON, FRP and DOP) for the full model. Notably, for NH₄ in Cluster 1, factors other than rainfall and runoff explained almost all the variability that
 345 could be captured by the BMA.

Table 4: Comparison between BMA performance using rainfall/runoff predictors only and all candidate predictors (full models).

Constituent	NSE for Cluster 1 (“wet”)			NSE for Cluster 2 (“dry”)		
	Rainfall, runoff only	Full model	% change in NSE	Rainfall, runoff only	Full model	% change in NSE
TSS	0.32	0.35	11	0.42	0.58	38
PN	0.32	0.40	24	0.38	0.59	56
NO _x	0.23	0.49	113	0.32	0.64	101
NH ₄	0.00	0.39	/	0.18	0.34	88
DON	0.20	0.37	84	0.20	0.43	117
FRP	0.27	0.45	68	0.26	0.40	56
DOP	0.00	0.04	/	0.22	0.62	181
PP	0.29	0.36	24	0.34	0.51	51
EC	0.41	0.68	66	0.39	0.54	39



4 Discussion

350 4.1 Factors influencing temporal variability in stream water quality

4.1.1 Runoff and rainfall

Our results demonstrated that runoff and rainfall were important factors in explaining the temporal dynamics of particulate pollutants (i.e. TSS, PN and PP) and dissolved species (e.g., NO_x, DOP and EC) in the GBR catchments. These results align with the findings of previous studies that have used these variables to understand changes in water quality over time (Beiter et al., 2020; Letcher et al., 2002; Liu et al., 2008b; McKergow et al., 2003; Schwarz et al., 2006; Tilburg et al., 2015).

Hydrologic and climatic variables (i.e. rainfall and runoff) showed distinct effects on different constituents, as well as different groups of catchments. The positive effect of event runoff and rainfall on sediment and particulate nutrients (i.e., PN, PP) revealed their underlying impacts on pollutant mobilisation and transport processes in catchments (Ballantine et al., 2009; Guo et al., 2010; Heathwaite et al., 2000; Hirsch et al., 2010; Lintern et al., 2018b; Musolff et al., 2015). In contrast, there were negative effects of during-event runoff on NO_x (Cluster 1), DOP (Cluster 2) and EC (both clusters). For NO_x and EC, this was most likely caused by hydrological transport processes; these constituents tend to be transported to receiving rivers via subsurface flows (Kratz et al., 1997; McKergow et al., 2003). For events with relatively low surface runoff, higher NO_x and EC event concentrations could be expected in these catchments (Clow and Sueker, 2000; Skoulikidis et al., 2006; Young et al., 1996). In addition, for DOP, in-stream biogeochemical cycling was likely to have caused the negative effect of event runoff. The events with low runoff, coupled with high temperatures (positive effect of event temperature for DOP Cluster 2, Figure B3 [a]) may relate to increases in the rate of P releases from organic forms at higher temperatures (Verheyen et al., 2015).

Post-event runoff (*Post_Q*) showed effects on specific constituents (e.g., NO_x, FRP and EC). Two alternative reasons might explain this. First, high post-event runoff may be an indicator of large baseflow contribution during the events (Cuomo and Guida, 2016). Therefore, as discussed in the above paragraph, constituents that can be transported through subsurface flows tend to be influenced by amount of runoff after event. Alternatively, it was significantly and positively correlated with other event characteristics and catchment biophysical conditions (e.g., vegetation cover, Figure B1). These inter-correlated factors together could have influenced pollutant source, mobilisation and delivery (see discussions below) (Granger et al., 2010; Lintern et al., 2018a).

375 4.1.2 Vegetation cover

Vegetation cover was another driving factor that was found to have influenced water quality dynamics; antecedent NDVI (*Ante_NDVI*) was included in the plausible models more frequently than event NDVI. The negative effect of antecedent



NDVI on particulate and dissolved nutrients (except DOP) was in line with previous studies that have found that NDVI was negatively correlated with these constituent concentrations in streams (Griffith et al., 2002; Liu et al., 2015; Masocha et al., 2017). An explanation for these results could be that high vegetation groundcover tended to stabilise the surface soil and reduce sediment losses by erosion (Meyer et al., 1997; Singh et al., 2008). In addition, vegetation nutrient assimilation and retention processes consumed nutrients in sediment and waterbodies, and these processes peaked in spring and early summer, typically before the wet season in the GBR catchments (Tabacchi et al., 2000; Uwimana et al., 2018; Vymazal, 2007).

The effect of antecedent NDVI varied among groups of constituents in Clusters 1 and 2. Specifically, it was a key predictor for NO_x, NH₄ and FRP for Cluster one, and almost all constituents for Cluster 2. This can be explained by the contrasting landscapes and climate of these two regions (Liu et al., 2018). In the dense, vegetation-covered catchments in Cluster 1 (i.e., the sites in the Wet Tropics), dissolved inorganic nutrient losses were likely due to more fertile soils (e.g., application of fertiliser on sugarcane) during the growing season (Hunter and Walton, 2008; McKergow et al., 2005a). Furthermore, denser natural vegetation cover (e.g., riparian vegetation and forest) could increase plant uptake and assimilation of dissolved nutrients compared to the sparse vegetation cover in the Dry Tropics (Cluster 2) region. Conversely, among Cluster 2 sites, vegetation coverage showed clear seasonal variation, which was linked closely to the seasonality in rainfall and grazing activity. Sediments and particulate pollutants were likely to be mobilized in grazed catchments (high rate of soil erosion) and delivered to streams via surface runoff (Ballantine et al., 2009; Neil et al., 2002; Turner et al., 2012). More importantly, high vegetation cover tended to mitigate mobilisation of pollutants, through stabilising the surface soil and such that reduces sediment losses from erosion (Meyer et al., 1997; Rey, 2004; Singh et al., 2008; Zorzal-Almeida et al., 2018).

4.1.3 Soil moisture and evapotranspiration

The results showed that soil moisture (SM) and actual evapotranspiration (AET) had a high impact on different constituents, particularly in the Cluster 2 catchments (e.g., antecedent soil moisture [DON and EC], antecedent AET [TSS and EC]). These two variables were inter-correlated and affect the hydrological cycle and vegetation cover (Correll, 1996; Correll and Weller, 1989; Legates et al., 2011). The results indicated that antecedent soil moisture had a negative effect on PN, NO_x, NH₄, DON, DOP and FRP. On one hand, this was expected as antecedent soil moisture was positively correlated with vegetation cover, and high soil moisture tends to reduce soil erosion and increase plant nutrient uptake. It may also be that soil water content affected soil microbial activity, influencing the biogeochemical processes in catchments, such as denitrification (Doran et al., 1988; Doran, 1980; Weier et al., 1993). The rate of denitrification was also enhanced under anoxic conditions, when soil moisture was high (Skopp et al., 1990; Zhu et al., 2018a). On the other hand, higher soil water can be associated with increased shallow subsurface flow and leaching of some constituents such as NO_x (Zhu et al., 2018b). This appears not to occur to a sufficient extent for it to over-ride other impacts of soil moisture.



4.1.4 Temperature

410 Our results suggested that average event temperature ($Event_T$) had a positive effect on NO_x , FRP, and DOP. This may be attributed to the strong negative cross-correlation between temperature and event runoff and antecedent vegetation condition (Figure B1). Rainfall during a warmer period might have been associated with less event runoff, resulting in higher event mean concentrations (Sect. 4.1.1). The effect of event temperature can be also attributed to the fact that the higher temperatures could lead to more recent mineralisation of nutrients, increasing readily transportable dissolved nutrient sources

415 (Liu et al., 2017; Wang et al., 2020). In addition, higher event temperature might be associated with higher pre-event temperature, resulting in poor groundcover, potentially lowering the dissolved nutrients losses through plant assimilation/uptake (Sect. 0) (Muro et al., 2018).

4.2 Predicting temporal variations in water quality

The Bayesian modelling framework in this study provided a useful tool to assess in-stream water quality dynamics. The models were able to explain more temporal variation in NO_x and EC than in other constituents. This is related to the sources and delivery processes of these two constituents. Anthropogenic inputs (e.g. agriculture) for NO_x , and large stores in groundwater together with limited geochemical transformation for EC (salts) suggested that temporal changes in event concentration could be well-captured by the changes in catchment hydroclimatic and vegetation conditions. In addition, NO_x and EC tend to be transported in subsurface flow pathways. The dynamics of catchment soil wetness and vegetation cover

425 have been previously linked to hydrological interactions between surface and subsurface flows (Ursino et al., 2004). The incorporation of soil moisture and vegetation cover into the Bayesian modelling framework more readily allowed the description of the main ecohydrological processes of these two constituents.

In contrast, model performance for DOP was poor in Cluster 1 catchments, which can be explained by two reasons. First, in the Wet Tropics catchments, DOP concentrations were generally stable, regardless of changes in flow, which can be explained by chemical exchange processes between water and sediment in stream (White et al., 1998). This means that the variability in DOP cannot be captured by the environmental variables considered here. Second, the poor performance might be attributed to the data set having fewer observations of DOP EMCs among Cluster 1 sites. There were only 66 observations, compared to the next lowest number of 167 (EC) among other constituents in the Cluster 1 catchments, which may not be sufficient to fully inform the model. This small sample size could have led to outcomes of: 1) poor mixing of

435 MCMC chains for inclusion variables (Figure B7 [a]), where no predictors showed predictive power; and 2) the BMA failed to identify the plausible models, since none of the candidate models had enough predictive power to fit the data well (Guthke, 2017; Höge et al., 2019). Continuous DOP monitoring would be required to achieve a better understanding of the factors driving temporal variation in this constituent.

Statistical modelling in hydrology or water quality is affected by uncertainty, only some of which can be characterised

440 within any particular modelling framework (Beck, 1987; Kavetski et al., 2006; Mantovan et al., 2006; Renard et al., 2010;



Yang et al., 2007). The Bayesian modelling framework used in this study incorporated the uncertainties in model selection (between-model), observations and model parameters (within-model) directly into the model predictions (Steel, 2019). This is a more comprehensive characterisation than in studies where model structures are assumed a priori. Reporting of predictive uncertainty of temporal variations in water quality also provided valuable information on the confidence in the averaged predictions. Nevertheless, limitations remain in the BMA approach which are important to understand. For example, for EC, there was a larger predictive uncertainty and larger uncertainty in posterior inclusion probability for each predictor from the robustness assessment than estimated in the fit to the complete data set. One limitation of BMA is that the posterior model probability could be sensitive to the specification of the parameter prior distribution (Fernandez et al., 2001). Specifying more informative priors on model parameters (i.e., inclusion variable I_n) would have the effect of restricting the set of candidate models (Eicher et al., 2011; Rockey et al., 2016). Indeed, several studies have compared different predictive performances of different prior specification of BMA coefficients and found that the choice of prior matters (Bayarri et al., 2012; Eicher et al., 2011; Liang et al., 2008). Future investigation of the sensitivity of prior distributions for BMA coefficients might achieve a reduction in predictive uncertainty and instability in posterior inclusion probabilities.

4.3 Management implications

The identification of key drivers of temporal variation in water quality can inform catchment water quality management. The results of this study showed that the effects of hydro-climatic drivers (e.g., rainfall and runoff) and vegetation cover varied among constituents and regions. This may allow funding bodies, such as government, regional natural resource management groups, to identify regions where land management and restoration would have a greater effect on mitigating sediments and nutrients export. The results suggested that, compared to wet catchments, maintaining vegetation ground cover in large dry grazed catchments (e.g., the Burdekin and Fitzroy catchments in Cluster 2) before the wet seasons could be an effective way of reducing sediment losses via erosion processes. These results are consistent with current, improved land management practices across the GBR catchments (Brodie et al., 2009; Brodie et al., 2012; Government, 2017; Hunter and Walton, 2008; Star et al., 2015). Management measures (e.g., establishment of wetlands, re-vegetation/rehabilitation of gully and stabilisation of river banks) can reduce sediment losses from hillslope and gully erosions (Koci et al., 2020; Loch, 2000; Sherriff et al., 2016; Wilkinson et al., 2018). In addition, catchment-specific management that accounts for temporal variation in catchment hydrological connectivity is required for the control of dissolved nutrients. Dominant flow pathways for dissolved nutrients can vary spatially and temporally. For example, subsurface flow in the Wet Tropics region have tended to transmit more dissolved nutrient, because prolonged wet conditions lead to this region that is more likely to be connected via lateral subsurface flow (Geng et al., 2017; Stieglitz et al., 2003). The enhanced mobilisation of leached dissolved nutrients from intensive cropping (e.g., sugarcane) from perched groundwater should be targeted in these catchments (Melland et al., 2012). Management practices, such as conservation tillage, and adaptation of '4R' concept (right source, right rate, right time, right place) for fertiliser application may help to minimise dissolved nitrogen losses (Cestti et al., 2003; Lintern et al., 2020; Merriman et al., 2009; Snyder, 2017).



5. Conclusions

475 This study provides a data-driven understanding of key drivers influencing the temporal variation in water quality. A
hierarchical Bayesian model averaging framework was used to identify the key environmental drivers and predict the water
quality dynamics at multiple catchments. Results showed that the temporal dynamics of water quality can be predicted well
using models considering the combined effects of hydroclimate and vegetation groundcover. The effects of key hydro-
climatic and vegetation conditions varied among different constituents, and across regions. This study reinforces the
480 importance of vegetation cover management as one key management response, especially for large grazed catchments.
Future investigation could involve the development of a spatio-temporal modelling framework to fully capture the water
quality dynamics. More importantly, it has continued to be challenging to prioritise management practices and evaluate the
effectiveness of the improved management interventions. Consequently, with more land management surveys and
continuous water quality monitoring data available, an extended temporal or spatio-temporal modelling framework could
485 potentially be used to assess if the success of the restoration measures.

Data availability

Water quality data that supported this study was available upon request from the Great Barrier Reef Catchment Loads
Monitoring Program (GBREvents@dsiti.qld.gov.au). Sources of explanatory variables were listed in Table 2.

Author contribution

490 All authors contributed to the design of the research. SL carried out data collation, performed the simulations and prepared
the manuscript with contributions from all co-authors. All authors contributed to the interpretation of the results and
provided feedback.

Competing interests

The authors declare that they have no conflict of interest.

495 Acknowledgements

This study was supported by the Australian Research Council (LP140100495), the Environment Protection Authority
Victoria, the Victorian Department of Environment, Land, Water and Planning, Bureau of Meteorology and Queensland
Department of Natural Resources, Mines and Energy. The author would like to acknowledge the efforts of the Queensland
Department of Environment and Science who provided the water quality monitoring data. The authors would also like to



500 offer sincere gratitude to Ms. Jie Jian for her assistance in geospatial database compilation. Dr. Paul Leahy, Mr. Malcolm
Watson, Dr. Ulrike Bende-Michl, Mr. Paul Wilson, and Ms. Belinda Thompson all of whom provided valuable advice in the
preparation of this manuscript.

References

- Alexander, R. B., Johnes, P. J., Boyer, E. W., and Smith, R. A.: A comparison of models for estimating the riverine export of nitrogen
505 from large watersheds, *Biogeochemistry*, 57, 295-339, 2002.
- Allan, D., Erickson, D., and Fay, J.: The influence of catchment land use on stream integrity across multiple spatial scales, *Freshwater
biology*, 37, 149-161, 1997.
- Ballantine, D., Walling, D. E., and Leeks, G. J.: Mobilisation and transport of sediment-associated phosphorus by surface runoff, *Water,
air, and soil pollution*, 196, 311-320, 2009.
- 510 Bartley, R., Speirs, W. J., Ellis, T. W., and Waters, D. K.: A review of sediment and nutrient concentration data from Australia for use in
catchment water quality models, *Marine pollution bulletin*, 65, 101-116, 2012.
- Bartley, R., Thompson, C., Croke, J., Pietsch, T., Baker, B., Hughes, K., and Kinsey-Henderson, A.: Insights into the history and timing of
post-European land use disturbance on sedimentation rates in catchments draining to the Great Barrier Reef, *Marine pollution bulletin*,
131, 530-546, 2018.
- 515 Beiter, D., Weiler, M., and Blume, T.: Characterising hillslope–stream connectivity with a joint event analysis of stream and groundwater
levels, *Hydrol. Earth Syst. Sci.*, 24, 5713-5744, 2020.
- Bhaduri, A., Bogardi, J., Siddiqi, A., Voigt, H., Vörösmarty, C., Pahl-Wostl, C., Bunn, S. E., Shrivastava, P., Lawford, R., and Foster, S.:
Achieving sustainable development goals from a water perspective, *Frontiers in Environmental Science*, 4, 64, 2016.
- Bieger, K., Hörmann, G., and Fohrer, N.: Simulation of streamflow and sediment with the soil and water assessment tool in a data scarce
520 catchment in the three Gorges region, China, *Journal of environmental quality*, 43, 37-45, 2014.
- Bouraoui, F., Galbiati, L., and Bidoglio, G.: Climate change impacts on nutrient loads in the Yorkshire Ouse catchment (UK), *Hydrology
and earth system sciences discussions*, 6, 197-209, 2002.
- Box, G. E. and Cox, D. R.: An analysis of transformations, *Journal of the Royal Statistical Society: Series B (Methodological)*, 26, 211-
243, 1964.
- 525 Brevik, E. C., Fenton, T. E., and Lazari, A.: Soil electrical conductivity as a function of soil water content and implications for soil
mapping, *Precision Agriculture*, 7, 393-404, 2006.
- Brodie, J., Lewis, S., Bainbridge, Z., Mitchell, A., Waterhouse, J., and Kroon, F.: Target setting for pollutant discharge management of
rivers in the Great Barrier Reef catchment area, *Marine and Freshwater Research*, 60, 1141-1149, 2009.
- Brodie, J. E., Kroon, F., Schaffelke, B., Wolanski, E., Lewis, S., Devlin, M., Bohnet, I., Bainbridge, Z., Waterhouse, J., and Davis, A.:
530 Terrestrial pollutant runoff to the Great Barrier Reef: an update of issues, priorities and management responses, *Marine Pollution Bulletin*,
65, 81-100, 2012.
- Bureau of Meteorology: Geofabric V2., 2012.
- Carpenter, S. R., Caraco, N. F., Correll, D. L., Howarth, R. W., Sharpley, A. N., and Smith, V. H.: Nonpoint pollution of surface waters
with phosphorus and nitrogen, *Ecological applications*, 8, 559-568, 1998.
- 535 Cestti, R., Srivastava, J. P., and Jung, S.: Agriculture Non-Point Source Pollution Control: Good Management Practices---The Chesapeake
Bay Experience, The World Bank, 2003.
- Chang, F.-J., Tsai, Y.-H., Chen, P.-A., Coynel, A., and Vachaud, G.: Modeling water quality in an urban river using hydrological factors–
Data driven approaches, *Journal of environmental management*, 151, 87-96, 2015.
- Clow, D. W. and Sueker, J. K.: Relations between basin characteristics and stream water chemistry in alpine/subalpine basins in Rocky
540 Mountain National Park, Colorado, *Water Resources Research*, 36, 49-61, 2000.
- Cooke, S. E., Ahmed, S. M., and MacAlpine, N.: Introductory guide to surface water quality monitoring in agriculture, Conservation and
Development Branch, Alberta Agriculture, Food and Rural ..., 2000.
- Correll, D.: Buffer zones and water quality protection: general principles, *Buffer zones: Their processes and potential in water protection*,
1996. 7-20, 1996.
- 545 Correll, D. L. and Weller, D. E.: Factors limiting processes in freshwater wetlands: an agricultural primary stream riparian forest,
Freshwater Wetlands and Wildlife, 1989. 1989.
- Cuomo, A. and Guida, D.: Using hydro-chemograph analyses to reveal runoff generation processes in a Mediterranean catchment,
Hydrological Processes, 30, 4462-4476, 2016.



- 550 Davis, A. M., Pearson, R. G., Brodie, J. E., and Butler, B.: Review and conceptual models of agricultural impacts and water quality in waterways of the Great Barrier Reef catchment area, *Marine and Freshwater Research*, 68, 1-19, 2017.
- Day, K. A. and McKeon, G. M.: An index of summer rainfall for Queensland's grazing lands, *Journal of Applied Meteorology and Climatology*, 57, 1623-1641, 2018.
- De Keersmaecker, W., Lhermitte, S., Tits, L., Honnay, O., Somers, B., and Coppin, P.: A model quantifying global vegetation resistance and resilience to short-term climate anomalies and their relationship with vegetation cover, *Global Ecology and Biogeography*, 24, 539-548, 2015.
- 555 de Mello, K., Valente, R. A., Randhir, T. O., dos Santos, A. C. A., and Vettorazzi, C. A.: Effects of land use and land cover on water quality of low-order streams in Southeastern Brazil: Watershed versus riparian zone, *Catena*, 167, 130-138, 2018.
- Deletic, A. B. and Maksimovic, C.: Evaluation of water quality factors in storm runoff from paved areas, *Journal of Environmental Engineering*, 124, 869-879, 1998.
- 560 Didan, K.: MOD13A2 MODIS/Terra Vegetation Indices 16-Day L3 Global 1km SIN Grid V006, NASA EOSDIS LP DAAC. 2015. DNRME: <https://water-monitoring.information.qld.gov.au/>, 2018.
- Doran, J., Mielke, L., and Stamatiadis, S.: Microbial activity and N cycling as regulated by soil water-filled pore space, 1988, 49-54.
- Doran, J. W.: Soil microbial and biochemical changes associated with reduced tillage 1, *Soil Science Society of America Journal*, 44, 765-771, 1980.
- 565 Fox, J., Weisberg, S., Adler, D., Bates, D., Baud-Bovy, G., Ellison, S., Firth, D., Friendly, M., Gorjanc, G., and Graves, S.: Package 'car', Vienna: R Foundation for Statistical Computing, 2012. 2012.
- French, R., Pilgrim, D., and Laurenson, B.: Experimental examination of the rational method for small rural catchments, 1974. 1974.
- Frost, A., Ramchurn, A., and Smith, A.: The Bureau's Operational AWRA Landscape (AWRA-L) Model, Melbourne, Bureau of Meteorology, 47, 2016.
- 570 Fu, B. and Burgher, I.: Riparian vegetation NDVI dynamics and its relationship with climate, surface water and groundwater, *Journal of Arid Environments*, 113, 59-68, 2015.
- Fu, B., Merritt, W. S., Croke, B. F., Weber, T., and Jakeman, A. J.: A review of catchment-scale water quality and erosion models and a synthesis of future prospects, *Environmental modelling & software*, 114, 75-97, 2019.
- Gelman, A., Stern, H. S., Carlin, J. B., Dunson, D. B., Vehtari, A., and Rubin, D. B.: Bayesian data analysis, Chapman and Hall/CRC, 2013.
- 575 Geng, X., Heiss, J. W., Michael, H. A., and Boufadel, M. C.: Subsurface flow and moisture dynamics in response to swash motions: Effects of beach hydraulic conductivity and capillarity, *Water Resources Research*, 53, 10317-10335, 2017.
- George, E. I. and McCulloch, R. E.: Variable selection via Gibbs sampling, *Journal of the American Statistical Association*, 88, 881-889, 1993.
- 580 Geoscience Australia: GEODATA 9 second DEM and D8: digital elevation model version 3 and flow direction grid 2008, Bioregion Assessment Source Dataset, 2008. 2008.
- Gilbert, M. and Brodie, J.: Population and major land use in the Great Barrier Reef catchment area spatial and temporal trends. Authority, G. B. R. M. P. (Ed.), Townsville, 2001.
- Gorman, D., Russell, B. D., and Connell, S. D.: Land-to-sea connectivity: linking human-derived terrestrial subsidies to subtidal habitat change on open rocky coasts, *Ecological Applications*, 19, 1114-1126, 2009.
- 585 Government, Q.: Reef 2050 Water Quality Improvement Plan - Management practices. Science, D. o. E. a. (Ed.), Brisbane, 2017.
- Granger, S., Bol, R., Anthony, S., Owens, P., White, S., and Haygarth, P.: Towards a holistic classification of diffuse agricultural water pollution from intensively managed grasslands on heavy soils. In: *Advances in Agronomy*, Elsevier, 2010.
- Griffith, J. A.: Geographic techniques and recent applications of remote sensing to landscape-water quality studies, *Water, Air, and Soil Pollution*, 138, 181-197, 2002.
- 590 Griffith, J. A., Martinko, E. A., Whistler, J. L., and Price, K. P.: Interrelationships among landscapes, NDVI, and stream water quality in the US Central Plains, *Ecological Applications*, 12, 1702-1718, 2002.
- Guo, D., Lintern, A., Webb, J. A., Ryu, D., Bende-Michl, U., Liu, S., and Western, A. W.: A data-based predictive model for spatiotemporal variability in stream water quality, *Hydrology and Earth System Sciences*, 24, 827-847, 2020.
- 595 Guo, D., Lintern, A., Webb, J. A., Ryu, D., Liu, S., Bende-Michl, U., Leahy, P., Wilson, P., and Western, A.: Key Factors Affecting Temporal Variability in Stream Water Quality, *Water Resources Research*, 55, 112-129, 2019.
- Guo, T., Wang, Q., Li, D., and Wu, L.: Sediment and solute transport on soil slope under simultaneous influence of rainfall impact and scouring flow, *Hydrological Processes: An International Journal*, 24, 1446-1454, 2010.
- Hawkins, D. and Weisberg, S.: Combining the box-cox power and generalised log transformations to accommodate nonpositive responses in linear and mixed-effects linear models, *South African Statistical Journal*, 51, 317-328, 2017.
- 600 Heathwaite, L., Sharpley, A., and Gburek, W.: A conceptual approach for integrating phosphorus and nitrogen management at watershed scales, *Journal of Environmental Quality*, 29, 158-166, 2000.
- Hem, J. D.: Fluctuations in concentration of dissolved solids of some southwestern streams, *Eos, Transactions American Geophysical Union*, 29, 80-84, 1948.



- 605 Hill, A. R.: Nitrate removal in stream riparian zones, *Journal of environmental quality*, 25, 743-755, 1996.
Hirsch, R. M., Moyer, D. L., and Archfield, S. A.: Weighted regressions on time, discharge, and season (WRTDS), with an application to Chesapeake Bay river inputs 1, *JAWRA Journal of the American Water Resources Association*, 46, 857-880, 2010.
Höge, M., Guthke, A., and Nowak, W.: The hydrologist's guide to Bayesian model selection, averaging and combination, *Journal of Hydrology*, 2019. 2019.
- 610 Hooten, M. B. and Hobbs, N. T.: A guide to Bayesian model selection for ecologists, *Ecological Monographs*, 85, 3-28, 2015.
Howarth, R. W., Sharpley, A., and Walker, D.: Sources of nutrient pollution to coastal waters in the United States: Implications for achieving coastal water quality goals, *Estuaries*, 25, 656-676, 2002.
Hunter, H. M. and Walton, R. S.: Land-use effects on fluxes of suspended sediment, nitrogen and phosphorus from a river catchment of the Great Barrier Reef, Australia, *Journal of Hydrology*, 356, 131-146, 2008.
- 615 Jarihani, B., Sidle, R., Bartley, R., Roth, C., and Wilkinson, S.: Characterisation of hydrological response to rainfall at multi spatio-temporal scales in savannas of semi-arid Australia, *Water*, 9, 540, 2017.
Joo, M., Raymond, M. A., McNeil, V. H., Huggins, R., Turner, R. D., and Choy, S.: Estimates of sediment and nutrient loads in 10 major catchments draining to the Great Barrier Reef during 2006–2009, *Marine pollution bulletin*, 65, 150-166, 2012.
- 620 Khan, U., Cook, F. J., Laugesen, R., Hasan, M. M., Plastow, K., Amirthanathan, G. E., Bari, M. A., and Tuteja, N. K.: Development of catchment water quality models within a realtime status and forecast system for the Great Barrier Reef, *Environmental Modelling & Software*, 132, 104790, 2020.
Kim, L.-H., Ko, S.-O., Jeong, S., and Yoon, J.: Characteristics of washed-off pollutants and dynamic EMCs in parking lots and bridges during a storm, *Science of the total environment*, 376, 178-184, 2007.
Koci, J., Sidle, R. C., Jarihani, B., and Cashman, M. J.: Linking hydrological connectivity to gully erosion in savanna rangelands tributary to the Great Barrier Reef using Structure-from-Motion photogrammetry, *Land Degradation & Development*, 2019. 2019.
- 625 Koci, J., Sidle, R. C., Kinsey-Henderson, A. E., Bartley, R., Wilkinson, S. N., Hawdon, A. A., Jarihani, B., Roth, C. H., and Hogarth, L.: Effect of reduced grazing pressure on sediment and nutrient yields in savanna rangeland streams draining to the Great Barrier Reef, *Journal of Hydrology*, 582, 124520, 2020.
Kohavi, R.: A study of cross-validation and bootstrap for accuracy estimation and model selection, 1995, 1137-1145.
- 630 Kratz, T., Webster, K., Bowser, C., Maguson, J., and Benson, B.: The influence of landscape position on lakes in northern Wisconsin, *Freshwater Biology*, 37, 209-217, 1997.
Kuhnert, P., Wang, Y.-G., Henderson, B., Stewart, L., and Wilkinson, S.: Statistical methods for the estimation of pollutant loads from monitoring data, Final Project Report. Report to the Marine and Tropical Sciences Research Facility, Reef and Rainforest Research Centre Limited, Cairns, 2009. 2009.
- 635 Lam, Q., Schmalz, B., and Fohrer, N.: Modelling point and diffuse source pollution of nitrate in a rural lowland catchment using the SWAT model, *Agricultural Water Management*, 97, 317-325, 2010.
Lawrance, A. J.: Regression transformation diagnostics using local influence, *Journal of the American Statistical Association*, 83, 1067-1072, 1988.
- Legates, D. R., Mahmood, R., Levia, D. F., DeLiberty, T. L., Quiring, S. M., Houser, C., and Nelson, F. E.: Soil moisture: A central and unifying theme in physical geography, *Progress in Physical Geography*, 35, 65-86, 2011.
- 640 Letcher, R. A., Jakeman, A. J., Calfas, M., Linforth, S., Baginska, B., and Lawrence, I.: A comparison of catchment water quality models and direct estimation techniques, *Environmental Modelling & Software*, 17, 77-85, 2002.
Link, W. A. and Barker, R. J.: Model weights and the foundations of multimodel inference, *Ecology*, 87, 2626-2635, 2006.
Lintern, A., McPhillips, L., Winfrey, B., Duncan, J., and Grady, C.: Best Management Practices for Diffuse Nutrient Pollution: Wicked Problems Across Urban and Agricultural Watersheds, *Environmental science & technology*, 54, 9159-9174, 2020.
- 645 Lintern, A., Webb, J., Ryu, D., Liu, S., Bende-Michl, U., Waters, D., Leahy, P., Wilson, P., and Western, A.: Key factors influencing differences in stream water quality across space, *Wiley Interdisciplinary Reviews: Water*, 5, e1260, 2018a.
Lintern, A., Webb, J., Ryu, D., Liu, S., Waters, D., Leahy, P., Bende-Michl, U., and Western, A.: What are the key catchment characteristics affecting spatial differences in riverine water quality?, *Water Resources Research*, 54, 7252-7272, 2018b.
- 650 Liu, S., Ryu, D., Webb, J., Lintern, A., Waters, D., Guo, D., and Western, A.: Characterisation of spatial variability in water quality in the Great Barrier Reef catchments using multivariate statistical analysis, *Marine Pollution Bulletin*, 137, 137-151, 2018.
Liu, W., Yao, L., Wang, Z., Xiong, Z., and Liu, G.: Human land uses enhance sediment denitrification and N₂O production in Yangtze lakes primarily by influencing lake water quality, *Biogeosciences*, 12, 6059-6070, 2015.
Liu, Y., Guo, H., Mao, G., and Yang, P.: A bayesian hierarchical model for urban air quality prediction under uncertainty, *Atmospheric Environment*, 42, 8464-8469, 2008a.
- 655 Liu, Y., Wang, C., He, N., Wen, X., Gao, Y., Li, S., Niu, S., Butterbach-Bahl, K., Luo, Y., and Yu, G.: A global synthesis of the rate and temperature sensitivity of soil nitrogen mineralization: latitudinal patterns and mechanisms, *Global change biology*, 23, 455-464, 2017.
Liu, Z. J., Weller, D. E., Jordan, T. E., Correll, D. L., and Boomer, K. B.: Integrated Modular Modeling of Water and Nutrients From Point and Nonpoint Sources in the Patuxent River Watershed. Wiley Online Library, 2008b.



- 660 Lloyd, C., Freer, J., Johnes, P., and Collins, A.: Using hysteresis analysis of high-resolution water quality monitoring data, including uncertainty, to infer controls on nutrient and sediment transfer in catchments, *Science of the Total Environment*, 543, 388-404, 2016.
- Loch, R.: Effects of vegetation cover on runoff and erosion under simulated rain and overland flow on a rehabilitated site on the Meandu Mine, Tarong, Queensland, *Soil Research*, 38, 299-312, 2000.
- Mainali, J. and Chang, H.: Landscape and anthropogenic factors affecting spatial patterns of water quality trends in a large river basin, South Korea, *Journal of hydrology*, 564, 26-40, 2018.
- 665 Mainali, J., Chang, H., and Chun, Y.: A review of spatial statistical approaches to modeling water quality, *Progress in Physical Geography: Earth and Environment*, 0, 0309133319852003, 2019.
- Masocha, M., Murwira, A., Magadza, C. H., Hirji, R., and Dube, T.: Remote sensing of surface water quality in relation to catchment condition in Zimbabwe, *Physics and Chemistry of the Earth, Parts A/B/C*, 100, 13-18, 2017.
- 670 McGrane, S. J.: Impacts of urbanisation on hydrological and water quality dynamics, and urban water management: a review, *Hydrological Sciences Journal*, 61, 2295-2311, 2016.
- McKergow, L. A., Prosser, I. P., Hughes, A. O., and Brodie, J.: Regional scale nutrient modelling: exports to the Great Barrier Reef world heritage area, *Marine pollution bulletin*, 51, 186-199, 2005a.
- McKergow, L. A., Prosser, I. P., Hughes, A. O., and Brodie, J.: Sources of sediment to the Great Barrier Reef world heritage area, *Marine pollution bulletin*, 51, 200-211, 2005b.
- 675 McKergow, L. A., Weaver, D. M., Prosser, I. P., Grayson, R. B., and Reed, A. E.: Before and after riparian management: sediment and nutrient exports from a small agricultural catchment, Western Australia, *Journal of Hydrology*, 270, 253-272, 2003.
- Melland, A., Mellander, P.-E., Murphy, P., Wall, D., Mechan, S., Shine, O., Shortle, G., and Jordan, P.: Stream water quality in intensive cereal cropping catchments with regulated nutrient management, *Environmental science & policy*, 24, 58-70, 2012.
- 680 Merriman, K. R., Gitau, M., and Chaubey, I.: A tool for estimating best management practice effectiveness in Arkansas, *Applied Engineering in Agriculture*, 25, 199-213, 2009.
- Meyer, D. L., Townsend, E. C., and Thayer, G. W.: Stabilization and erosion control value of oyster cultch for intertidal marsh, *Restoration Ecology*, 5, 93-99, 1997.
- Miller, C., Magdalina, A., Willows, R., Bowman, A., Scott, E., Lee, D., Burgess, C., Pope, L., Pannullo, F., and Haggarty, R.: Spatiotemporal statistical modelling of long-term change in river nutrient concentrations in England & Wales, *Science of the Total Environment*, 466, 914-923, 2014.
- 685 Muro, J., Strauch, A., Heinemann, S., Steinbach, S., Thonfeld, F., Waske, B., and Diekkrüger, B.: Land surface temperature trends as indicator of land use changes in wetlands, *International journal of applied earth observation and geoinformation*, 70, 62-71, 2018.
- Murphy, B. F. and Ribbe, J.: Variability of southeastern Queensland rainfall and climate indices, *International Journal of Climatology: A Journal of the Royal Meteorological Society*, 24, 703-721, 2004.
- 690 Musolff, A., Schmidt, C., Selle, B., and Fleckenstein, J. H.: Catchment controls on solute export, *Advances in Water Resources*, 86, 133-146, 2015.
- Nash, J. E. and Sutcliffe, J. V.: River flow forecasting through conceptual models part I—A discussion of principles, *Journal of hydrology*, 10, 282-290, 1970.
- 695 Neil, D. T., Orpin, A. R., Ridd, P. V., and Yu, B.: Sediment yield and impacts from river catchments to the Great Barrier Reef lagoon: a review, *Marine and Freshwater Research*, 53, 733-752, 2002.
- Noori, N., Kalin, L., and Isik, S.: Water quality prediction using SWAT-ANN coupled approach, *Journal of Hydrology*, 590, 125220, 2020.
- Novotny, V.: Diffuse pollution from agriculture—a worldwide outlook, *Water Science and Technology*, 39, 1-13, 1999.
- 700 Ntzoufras, I.: Gibbs variable selection using BUGS, *Journal of statistical software*, 7, 1-19, 2002.
- O'Hara, R. B. and Sillanpää, M. J.: A review of Bayesian variable selection methods: what, how and which, *Bayesian analysis*, 4, 85-117, 2009.
- Orr, D., Turner, R. D. R., Huggins, R., Vardy, S., and J., W. M. S.: Wet Tropics water quality statistics for high and base flow conditions., *Great Barrier Reef Catchment Loads Monitoring Program*, D. o. S., Information and Technology, I. a. t. A. (Eds.), Brisbane, 2014.
- 705 Paliwal, R., Sharma, P., and Kansal, A.: Water quality modelling of the river Yamuna (India) using QUAL2E-UNCAS, *Journal of environmental management*, 83, 131-144, 2007.
- Papagiannopoulou, C., Miralles, D., Dorigo, W. A., Verhoest, N., Depoorter, M., and Waegeman, W.: Vegetation anomalies caused by antecedent precipitation in most of the world, *Environmental Research Letters*, 12, 074016, 2017.
- Peel, M. C., Finlayson, B. L., and McMahon, T. A.: Updated world map of the Köppen-Geiger climate classification, *Hydrology and earth system sciences discussions*, 4, 439-473, 2007.
- 710 Pérez-Gutiérrez, J. D., Paz, J. O., and Tagert, M. L. M.: Seasonal water quality changes in on-farm water storage systems in a south-central US agricultural watershed, *Agricultural water management*, 187, 131-139, 2017.
- Peters, N. E. and Meybeck, M.: Water quality degradation effects on freshwater availability: impacts of human activities, *Water International*, 25, 185-193, 2000.



- 715 Pilgrim, E., Institution of Engineers, A., Pilgrim, D., and Canterford, R.: Australian rainfall and runoff, Institution of Engineers, Australia, 1987.
Plummer, M.: JAGS: A program for analysis of Bayesian graphical models using Gibbs sampling, 2003.
Plummer, M.: JAGS: Just another Gibbs sampler, version 3.4.0, URL <http://mcmc-jags.sourceforge.net>, 2013a. 2013a.
Plummer, M.: rjags: Bayesian graphical models using MCMC, R package version, 3, 2013b.
- 720 Pretty, J., Hildrew, A., and Trimmer, M.: Nutrient dynamics in relation to surface–subsurface hydrological exchange in a groundwater fed chalk stream, *Journal of Hydrology*, 330, 84-100, 2006.
R Core Team: R: A language and environment for statistical computing, 2013. 2013.
Raftery, A. E., Madigan, D., and Hoeting, J. A.: Bayesian model averaging for linear regression models, *Journal of the American Statistical Association*, 92, 179-191, 1997.
- 725 Raupach, M., Briggs, P., Haverd, V., King, E., Paget, M., and Trudinger, C.: Australian water availability project (AWAP): CSIRO marine and atmospheric research component: final report for phase 3, Melbourne: Centre for Australian weather and climate research (bureau of meteorology and CSIRO), 67, 2009.
Ren, W., Zhong, Y., Meligrana, J., Anderson, B., Watt, W. E., Chen, J., and Leung, H.-L.: Urbanization, land use, and water quality in Shanghai: 1947–1996, *Environment International*, 29, 649-659, 2003.
- 730 Rey, F.: Effectiveness of vegetation barriers for marly sediment trapping, *Earth Surface Processes and Landforms: The Journal of the British Geomorphological Research Group*, 29, 1161-1169, 2004.
Richards, R. P. and Baker, D. B.: Trends in nutrient and suspended sediment concentrations in Lake Erie tributaries, 1975–1990, *Journal of Great Lakes Research*, 19, 200-211, 1993.
Rode, M., Arhonditsis, G., Balin, D., Kebede, T., Krysanova, V., Van Griensven, A., and Van der Zee, S. E.: New challenges in integrated water quality modelling, *Hydrological Processes*, 24, 3447-3461, 2010.
- 735 Schwarz, G., Hoos, A., Alexander, R., and Smith, R.: The SPARROW surface water-quality model: theory, application and user documentation, US geological survey techniques and methods report, book, 6, 2006.
Sharpley, A.: Managing agricultural phosphorus to minimize water quality impacts, *Scientia Agricola*, 73, 1-8, 2016.
Sherriff, S., Rowan, J., Melland, A., Jordan, P., Fenton, O., and O hUallachain, D.: Investigating suspended sediment dynamics in contrasting agricultural catchments using ex situ turbidity-based suspended sediment monitoring, *Hydrology and Earth System Sciences*, 19, 3349-3363, 2015.
- 740 Sherriff, S. C., Rowan, J. S., Fenton, O., Jordan, P., Melland, A. R., Mellander, P.-E., and Huallachain, D. O.: Storm event suspended sediment-discharge hysteresis and controls in agricultural watersheds: implications for watershed scale sediment management, *Environmental science & technology*, 50, 1769-1778, 2016.
- 745 Shi, P., Zhang, Y., Li, Z., Li, P., and Xu, G.: Influence of land use and land cover patterns on seasonal water quality at multi-spatial scales, *Catena*, 151, 182-190, 2017.
Singh, A., Jakubowski, A. R., Chidister, I., and Townsend, P. A.: A MODIS approach to predicting stream water quality in Wisconsin, *Remote Sensing of Environment*, 128, 74-86, 2013.
Singh, P., Bhunya, P., Mishra, S., and Chaube, U.: A sediment graph model based on SCS-CN method, *Journal of Hydrology*, 349, 244-255, 2008.
- 750 Skopp, J., Jawson, M., and Doran, J.: Steady-state aerobic microbial activity as a function of soil water content, *Soil Science Society of America Journal*, 54, 1619-1625, 1990.
Skoulikidis, N. T., Amaxidis, Y., Bertahas, I., Laschou, S., and Gritzalis, K.: Analysis of factors driving stream water composition and synthesis of management tools—a case study on small/medium Greek catchments, *Science of the Total Environment*, 362, 205-241, 2006.
- 755 Snyder, C. S.: Enhanced nitrogen fertiliser technologies support the ‘4R’ concept to optimise crop production and minimise environmental losses, *Soil Research*, 55, 463-472, 2017.
Star, M., Rolfe, J., Long, P., Whish, G., and Donaghy, P.: Improved grazing management practices in the catchments of the Great Barrier Reef, Australia: does climate variability influence their adoption by landholders?, *The Rangeland Journal*, 37, 507-515, 2015.
- 760 Stieglitz, M., Shaman, J., McNamara, J., Engel, V., Shanley, J., and Kling, G. W.: An approach to understanding hydrologic connectivity on the hillslope and the implications for nutrient transport, *Global biogeochemical cycles*, 17, 2003.
Tabacchi, E., Lambs, L., Guilloy, H., Planty-Tabacchi, A. M., Muller, E., and Decamps, H.: Impacts of riparian vegetation on hydrological processes, *Hydrological processes*, 14, 2959-2976, 2000.
Tang, W. and Carey, S. K.: HydRun: A MATLAB toolbox for rainfall–runoff analysis, *Hydrological Processes*, 31, 2670-2682, 2017.
- 765 Thompson, S., Basu, N., Lascrain, J., Aubeneau, A., and Rao, P.: Relative dominance of hydrologic versus biogeochemical factors on solute export across impact gradients, *Water Resources Research*, 47, 2011.
Tilburg, C. E., Jordan, L. M., Carlson, A. E., Zeeman, S. I., and Yund, P. O.: The effects of precipitation, river discharge, land use and coastal circulation on water quality in coastal Maine, *Royal Society open science*, 2, 140429, 2015.
Turner, R., Huggins, R., Wallace, R., Smith, R., Vardy, S., and Warne, M. S. J.: Sediment, Nutrient and Pesticide Loads: Great Barrier Reef Catchment Loads Monitoring 2009-2010, Department of Science, Information Technology, Innovation and the Arts, Brisbane, 2012.
- 770 53, 2012.



- Tweed, S. O., Leblanc, M., Webb, J. A., and Lubczynski, M. W.: Remote sensing and GIS for mapping groundwater recharge and discharge areas in salinity prone catchments, southeastern Australia, *Hydrogeology Journal*, 15, 75-96, 2007.
- Ustaoglu, F., Tepe, Y., and Taş, B.: Assessment of stream quality and health risk in a subtropical Turkey river system: A combined approach using statistical analysis and water quality index, *Ecological Indicators*, 113, 105815, 2020.
- 775 Uwimana, A., van Dam, A. A., Gettel, G. M., and Irvine, K.: Effects of agricultural land use on sediment and nutrient retention in valley-bottom wetlands of Migina catchment, southern Rwanda, *Journal of environmental management*, 219, 103-114, 2018.
- Varanou, E., Gkouvatou, E., Baltas, E., and Mimikou, M.: Quantity and quality integrated catchment modeling under climate change with use of soil and water assessment tool model, *Journal of Hydrologic Engineering*, 7, 228-244, 2002.
- 780 Verheyen, D., Van Gaelen, N., Ronchi, B., Batelaan, O., Struyf, E., Govers, G., Merckx, R., and Diels, J.: Dissolved phosphorus transport from soil to surface water in catchments with different land use, *Ambio*, 44, 228-240, 2015.
- Vymazal, J.: Removal of nutrients in various types of constructed wetlands, *Science of the total environment*, 380, 48-65, 2007.
- Walling, D.: Dissolved loads and their measurement, *Erosion and Sediment Yield: Some Methods of Measurement and Modelling*. Geo Books, Regency House Norwich(England). 1984. p 111-177, 18 fig, 10 tab, 104 ref., 1984. 1984.
- 785 Walling, D. and Foster, I.: Variations in the natural chemical concentration of river water during flood flows, and the lag effect: some further comments, *Journal of Hydrology*, 26, 237-244, 1975.
- Wan, Y., Qian, Y., Migliaccio, K. W., Li, Y., and Conrad, C.: Linking spatial variations in water quality with water and land management using multivariate techniques, *Journal of environmental quality*, 43, 599-610, 2014.
- Wang, A., Yang, D., and Tang, L.: Spatiotemporal variation in nitrogen loads and their impacts on river water quality in the upper Yangtze River basin, *Journal of Hydrology*, 590, 125487, 2020.
- 790 Wang, G., Jager, H. I., Baskaran, L. M., Baker, T. F., and Brandt, C. C.: SWAT modeling of water quantity and quality in the Tennessee river basin: spatiotemporal calibration and validation, *Hydrology and Earth System Sciences Discussions*, 2016. 1-33, 2016.
- Wang, Q., Schepen, A., and Robertson, D. E.: Merging seasonal rainfall forecasts from multiple statistical models through Bayesian model averaging, *Journal of Climate*, 25, 5524-5537, 2012.
- 795 Waterhouse, J., Schaffelke, B., Bartley, R., Eberhadr, R., Brodie, J., Star, M., Thorburn, P., Rolfe, J., Ronan, M., Taylor, B., and Kroon, F.: 2017 Scientific Consensus Statement: A synthesis of the science of land-based water quality impacts on the Great Barrier Reef., Department of the Premier and Cabinet, Q. G., Brisbane (Ed.), Brisbane, 2017.
- Waters, D., Carroll, C., Ellis, R., Hateley, L., McCloskey, J., Packett, R., Dougall, C., and Fentic, B.: Modelling reductions of pollutant loads due to improved management practices in the Great Barrier Reef Catchments-Whole of GBR, Volume 1 Department of Natural Resources and Mines, Technical Report (ISBN: 978-1-7423-0999), 2013.
- 800 Waters, D. and Packett, R.: Sediment and nutrient generation rates for Queensland rural catchments-an event monitoring program to improve water quality modelling, 2007.
- Webb, A. and King, E. L.: A Bayesian hierarchical trend analysis finds strong evidence for large-scale temporal declines in stream ecological condition around Melbourne, Australia, *Ecography*, 32, 215-225, 2009.
- 805 Weier, K., Doran, J., Power, J., and Walters, D.: Denitrification and the dinitrogen/nitrous oxide ratio as affected by soil water, available carbon, and nitrate, *Soil Science Society of America Journal*, 57, 66-72, 1993.
- Whistler, J.: A phenological approach to land cover characterization using Landsat MSS data for analysis of nonpoint source pollution, *KARS Rep*, 96, 1-59, 1996.
- 810 Wilkinson, S. N., Kinsey-Henderson, A. E., Hawdon, A. A., Hairsine, P. B., Bartley, R., and Baker, B.: Grazing impacts on gully dynamics indicate approaches for gully erosion control in northeast Australia, *Earth Surface Processes and Landforms*, 43, 1711-1725, 2018.
- Wintle, B. A., McCarthy, M. A., Volinsky, C. T., and Kavanagh, R. P.: The use of Bayesian model averaging to better represent uncertainty in ecological models, *Conservation biology*, 17, 1579-1590, 2003.
- Yang, J.-L., Zhang, G.-L., Shi, X.-Z., Wang, H.-J., Cao, Z.-H., and Ritsema, C. J.: Dynamic changes of nitrogen and phosphorus losses in ephemeral runoff processes by typical storm events in Sichuan Basin, Southwest China, *Soil and Tillage Research*, 105, 292-299, 2009.
- 815 Young, W. J., Marston, F. M., and Davis, R. J.: Nutrient exports and land use in Australian catchments, *Journal of environmental management*, 47, 165-183, 1996.
- Zhang, Q. and Blomquist, J. D.: Watershed export of fine sediment, organic carbon, and chlorophyll-a to Chesapeake Bay: spatial and temporal patterns in 1984-2016, *Science of the Total Environment*, 619, 1066-1078, 2018.
- 820 Zhang, Q., Harman, C. J., and Ball, W. P.: An improved method for interpretation of riverine concentration-discharge relationships indicates long-term shifts in reservoir sediment trapping, *Geophysical Research Letters*, 43, 10,215-210,224, 2016.
- Zhang, T. and Yang, B.: Box-cox transformation in big data, *Technometrics*, 59, 189-201, 2017.
- Zhang, Y.-K. and Schilling, K.: Temporal variations and scaling of streamflow and baseflow and their nitrate-nitrogen concentrations and loads, *Advances in Water Resources*, 28, 701-710, 2005.
- 825 Zhang, Y., Guo, F., Meng, W., and Wang, X.-Q.: Water quality assessment and source identification of Daliao river basin using multivariate statistical methods, *Environmental monitoring and assessment*, 152, 105, 2009.



- Zhu, G., Wang, S., Wang, C., Zhou, L., Zhao, S., Li, Y., Li, F., Jetten, M. S., Lu, Y., and Schwark, L.: Resuscitation of anammox bacteria after > 10,000 years of dormancy, *The ISME journal*, 2018a. 2018a.
- Zhu, Q., Castellano, M. J., and Yang, G.: Coupling soil water processes and nitrogen cycle across spatial scales: Potentials, bottlenecks and solutions, *Earth-science reviews*, 2018b. 2018b.
- 830 Zorzal-Almeida, S., Salim, A., Andrade, M. R. M., de Novaes Nascimento, M., Bini, L. M., and Bicudo, D. C.: Effects of land use and spatial processes in water and surface sediment of tropical reservoirs at local and regional scales, *Science of the total environment*, 644, 237-246, 2018.



Appendix A - Text

835 Hierarchical prior specification and Bayesian inference of key drivers

Bayesian inference required specification of prior distributions for each model parameter. A minimally-informative uniform prior (denote as $U(\cdot)$) between 0 and 10 was assigned to the global standard deviation (σ , Eq. A1) (Gelman, 2006). The prior of I_n assumes that each indicator comes from an independent Bernoulli distribution, with a probability of 0.5 (Eq. A2) (Raftery et al., 1997). This vague prior results in each model structure having an equal prior model probability.

$$\sigma \sim U(0,10) \quad \text{A1}$$

$$I_n \sim \text{Bernoulli}(0.5) \quad \text{A2}$$

840 We used a hierarchical conditional prior specification for predictor coefficients, allowing the site-specific parameter values that describe the effects of each temporal predictors ($\beta_{1,j}, \beta_{2,j}, \dots, \beta_{n,j}$) to be exchangeable between sites (Liu et al., 2008; O'Hara and Sillanpää, 2009; Webb and King, 2009). The prior of $\beta_{n,j}$ was conditioned on I_n , resulting in a mixture distribution with 'slab and spike' prior, which was defined as follows,

$$\beta_{n,j} | I_n \sim I_n N(0, \tau_n) + (1 - I_n) N(0, \tau_{n,tune}) \quad \text{A3}$$

845 where $\beta_{n,j} | (I_n = 1)$ is the slab part of the mixture distribution. The $\beta_{n,j} | (I_n = 1)$ was estimated by including a higher-level distribution. The prior of $\beta_{n,j} | (I_n = 1)$ followed a normal distribution with random effect (Eq. A4), with the τ_n drawn from a common prior distribution, defined as a hyperparameter (i.e., uniform distribution between 0 to 20, Eq. A5) (Gelman, 2006; Kruschke, 2014).

$$\beta_{n,j} | (I_n = 1) \sim N(0, \tau_n) \quad \text{A4}$$

$$\tau_n \sim U(0, 20) \quad \text{A5}$$

For the spike component, a data-dependent prior was specified for $\beta_{n,j} | (I_n = 0)$, drawing from a *pseudo-prior* (Eq. A6), that is, a *prior* distribution with no effect on the posterior distribution, but facilitating the mixing of the Gibbs sampler.

$$\beta_{n,j} | (I_n = 0) \sim N(0, \tau_{n,tune}) \quad \text{A6}$$

850 We estimated $\tau_{n,tune}$ from the standard deviations of the posterior of the $\beta_{n,j}$ in a global model structure (i.e., modelling structure using all predictors), as suggested by Carlin and Chib (1995) and Linden and Roloff (2015). The prior of $\beta_{n,j} | (I_n = 0)$ was near the posterior estimates to facilitate mixing in the MCMC (Hooten and Hobbs, 2015).

The posterior inclusion probability (PIP - $P(I_n = 1 | \mathbf{y})$, Eq.A7) of each predictor was used to compare the relative importance of individual predictors (i.e., how often the n^{th} predictor was 'in' the model).

$$P(I_n = 1 | \mathbf{y}) = \frac{1}{T} \sum_{t=1}^T I(I_n^{(t)} = 1) \quad \text{A7}$$



855 where T is the total number of iterations of Markov chains. The different combination of I_n at each MCMC sampling represents a specific model structure. According to Bayes' theorem, the posterior model probability (PMP - $P(M_k|\mathbf{y})$) can be estimated as,

$$P(M_k | \mathbf{y}) = \frac{[\mathbf{y}|M_k]P(M_k)}{\sum_{x=1}^L [\mathbf{y}|M_x]P(M_x)} \quad \text{A8}$$

where L is the total number of possible models, and $P(M_k)$ is the prior probability of model M_k , among a group of models M_x , $x = 1, \dots, X$. This posterior model probability can be obtained by assessing the frequency of a particular combination of I_n
860 during the MCMC sampling.

Reference

- Carlin, B. P. and Chib, S.: Bayesian model choice via Markov chain Monte Carlo methods, *Journal of the Royal Statistical Society: Series B (Methodological)*, 57, 473-484, 1995.
- 865 Gelman, A.: Prior distributions for variance parameters in hierarchical models (comment on article by Browne and Draper), *Bayesian analysis*, 1, 515-534, 2006.
- Hooten, M. B. and Hobbs, N. T.: A guide to Bayesian model selection for ecologists, *Ecological Monographs*, 85, 3-28, 2015.
- Kruschke, J.: *Doing Bayesian data analysis: A tutorial with R, JAGS, and Stan*, Academic Press, 2014.
- Linden, D. W. and Roloff, G. J.: Improving inferences from short-term ecological studies with Bayesian hierarchical modeling: white-headed woodpeckers in managed forests, *Ecology and evolution*, 5, 3378-3388, 2015.
- 870 Liu, Y., Guo, H., Mao, G., and Yang, P.: A bayesian hierarchical model for urban air quality prediction under uncertainty, *Atmospheric Environment*, 42, 8464-8469, 2008.
- O'Hara, R. B. and Sillanpää, M. J.: A review of Bayesian variable selection methods: what, how and which, *Bayesian analysis*, 4, 85-117, 2009.
- 875 Raftery, A. E., Madigan, D., and Hoeting, J. A.: Bayesian model averaging for linear regression models, *Journal of the American Statistical Association*, 92, 179-191, 1997.
- Webb, A. and King, E. L.: A Bayesian hierarchical trend analysis finds strong evidence for large-scale temporal declines in stream ecological condition around Melbourne, Australia, *Ecography*, 32, 215-225, 2009.

880



Appendix B - Figure

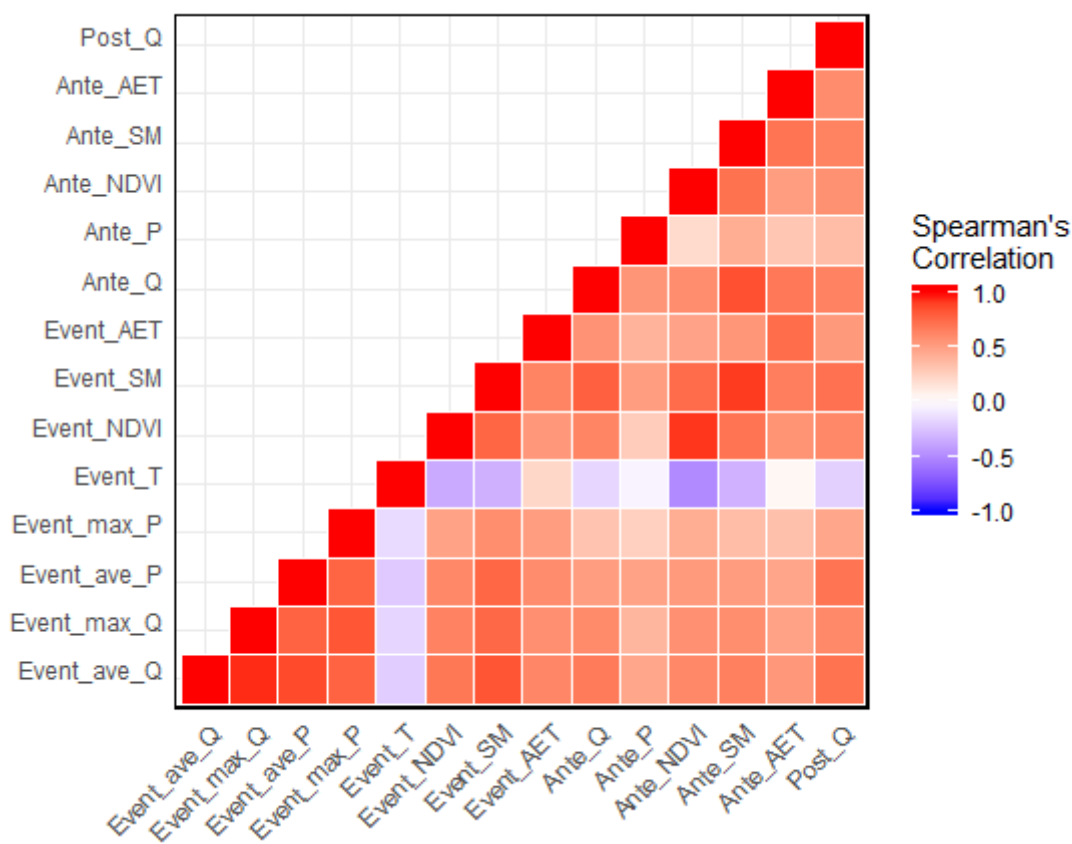
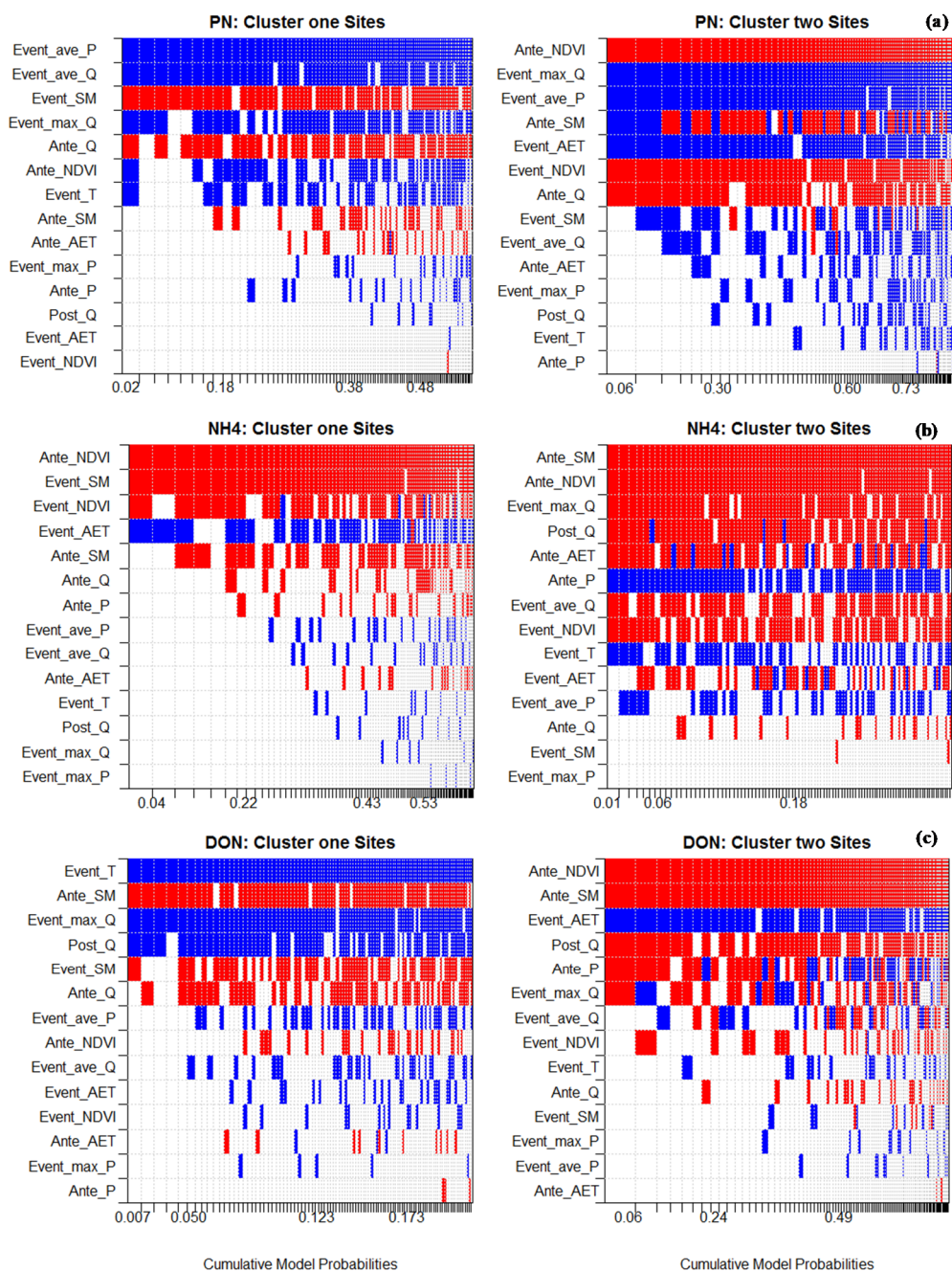


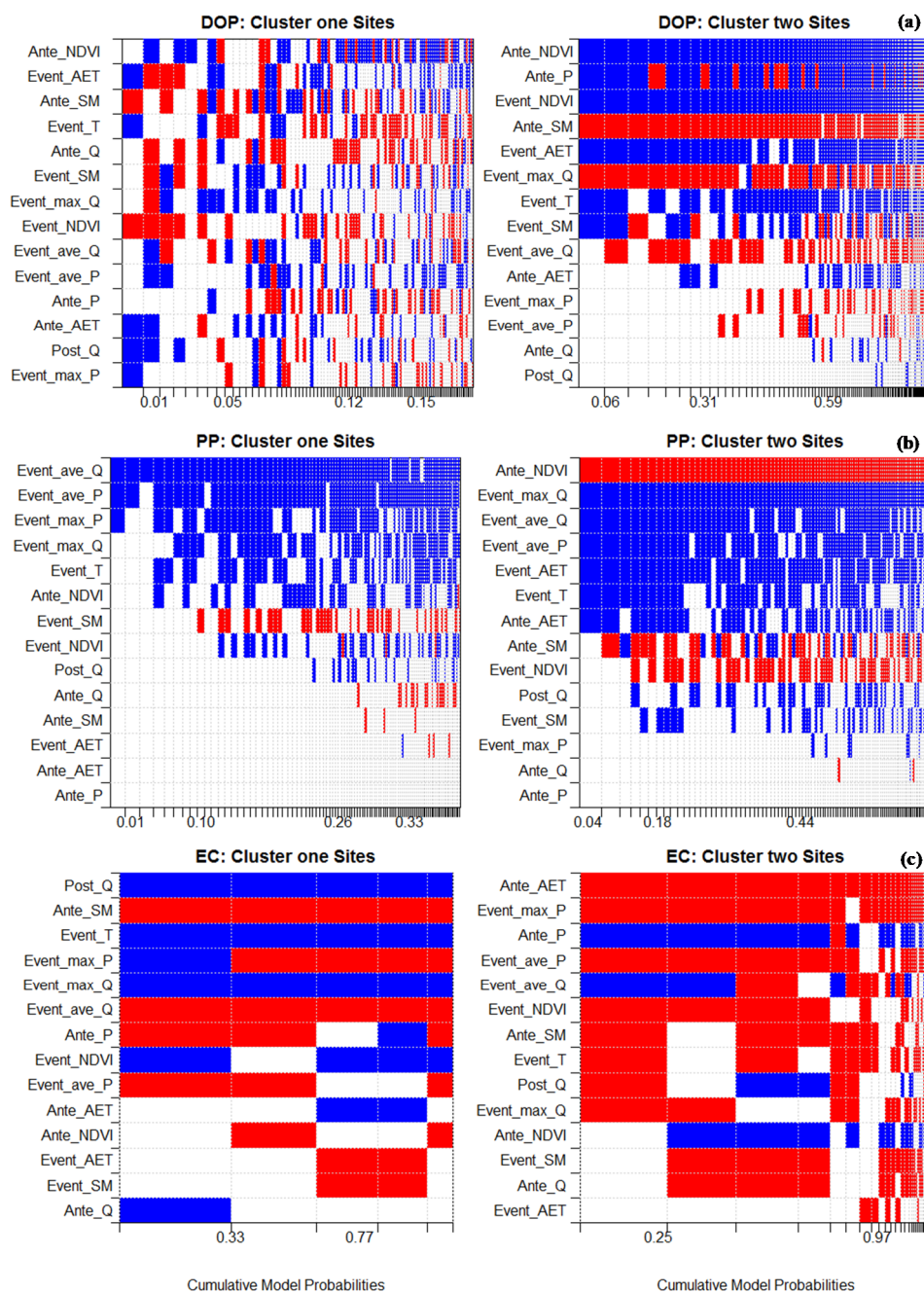
Figure B1: Spearman's Rank correlation between 14 candidate covariates.

885

890



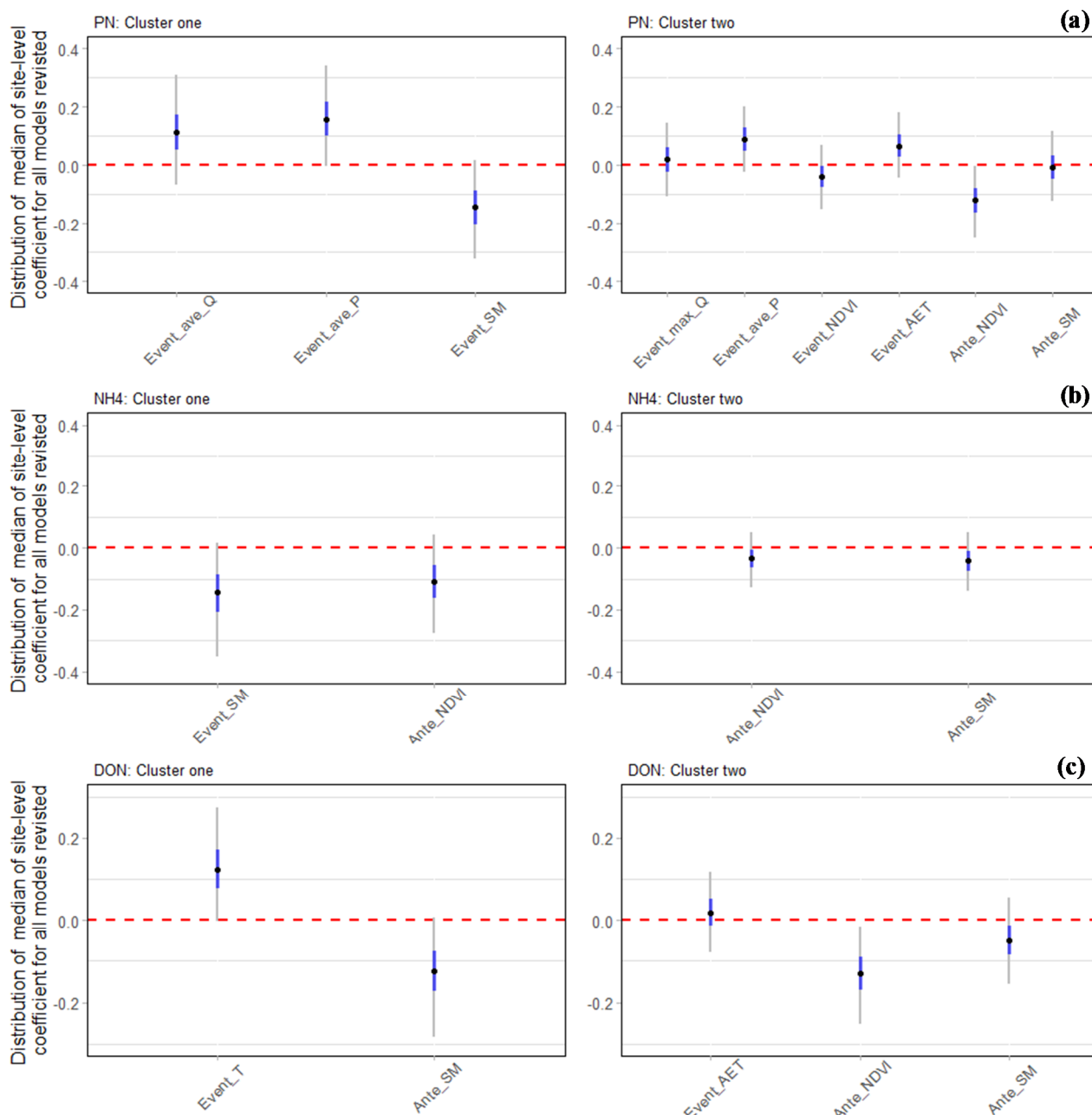
895 **Figure B2: Comparison of BMA model coefficient and cumulative model probability (top 100 models) between two clusters for: (a) PN, (b) NH₄ and (c) DON. Left - cluster one sites and Right – cluster two sites. The order of predictors on the y-axis was ranked based on the posterior inclusion probability. Each column in the heatmap represents the one specific model (ranked from highest model probability) and the width of the column is normalised by the posterior model probability. The colour indicates the direction of the coefficients, red – negative and blue – positive. Note: the coefficient value was averaged across the posterior median value of site-specific coefficient within each cluster (effect size, θ_{nj} , in Eq. (6)).**



900

Figure B3: Comparison of BMA model coefficient and cumulative model probability (top 100 models) between two clusters for: (a) DOP, (b) PP and (c) EC. Left - cluster one sites and Right – cluster two sites. The order of predictors on the y-axis was ranked based on the posterior inclusion probability. Each column in the heatmap represents the one specific model (ranked from highest model probability) and the width of the column is normalised by the posterior model probability. The colour indicates the direction of the coefficients, red – negative and blue – positive. Note: the coefficient value was averaged across the posterior median value of site-specific coefficient within each cluster (effect size, θ_{nj} , in Eq. (6)).

905



910 **Figure B4: Distribution of median of site-level coefficients for all plausible models in BMA. (a) PN, (b) NH₄ and (c) DON. Only predictors with PIP > 0.8 are included. For each specific model structure, the coefficient value of a predictor was the median of site-specific coefficient across all sites (effect size, θ_{nj} in Eq. (6)). The distribution of this value thus represents the probability of the model (PMP), as well as variability in the same predictor across different sites. Note: black dots indicate the median; grey**



vertical lines indicate 95% CI and blue coloured vertical lines indicates 50% CI. The definition of abbreviation of each predictor can be found in Table 3.

915

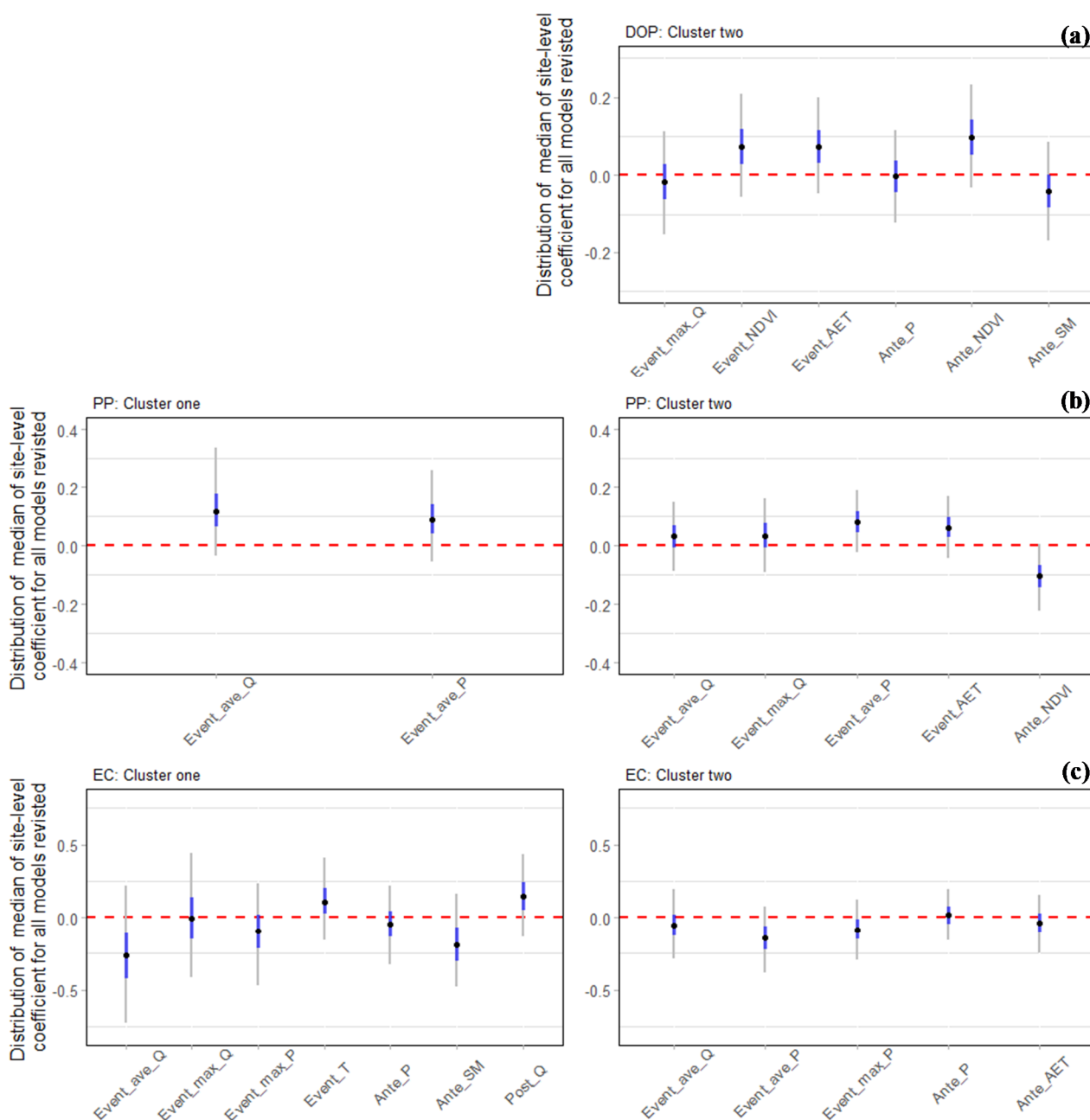


Figure B5: Distribution of median of site-level coefficients for all plausible models in BMA. (a) DOP, (b) PP and (c) EC. Only predictors with PIP > 0.8 are included. For each specific model structure, the coefficient value of a predictor was the median of



920 site-specific coefficient across all sites (effect size, $\theta_{n,j}$, in Equation 6). The distribution of this value thus represents the probability of the model (PMP), as well as variability in the same predictor across different sites. Note: black dots indicate the median; grey vertical lines indicate 95% CI and blue coloured vertical lines indicates 50% CI. The definition of abbreviation of each predictor can be found in Table 3.

925

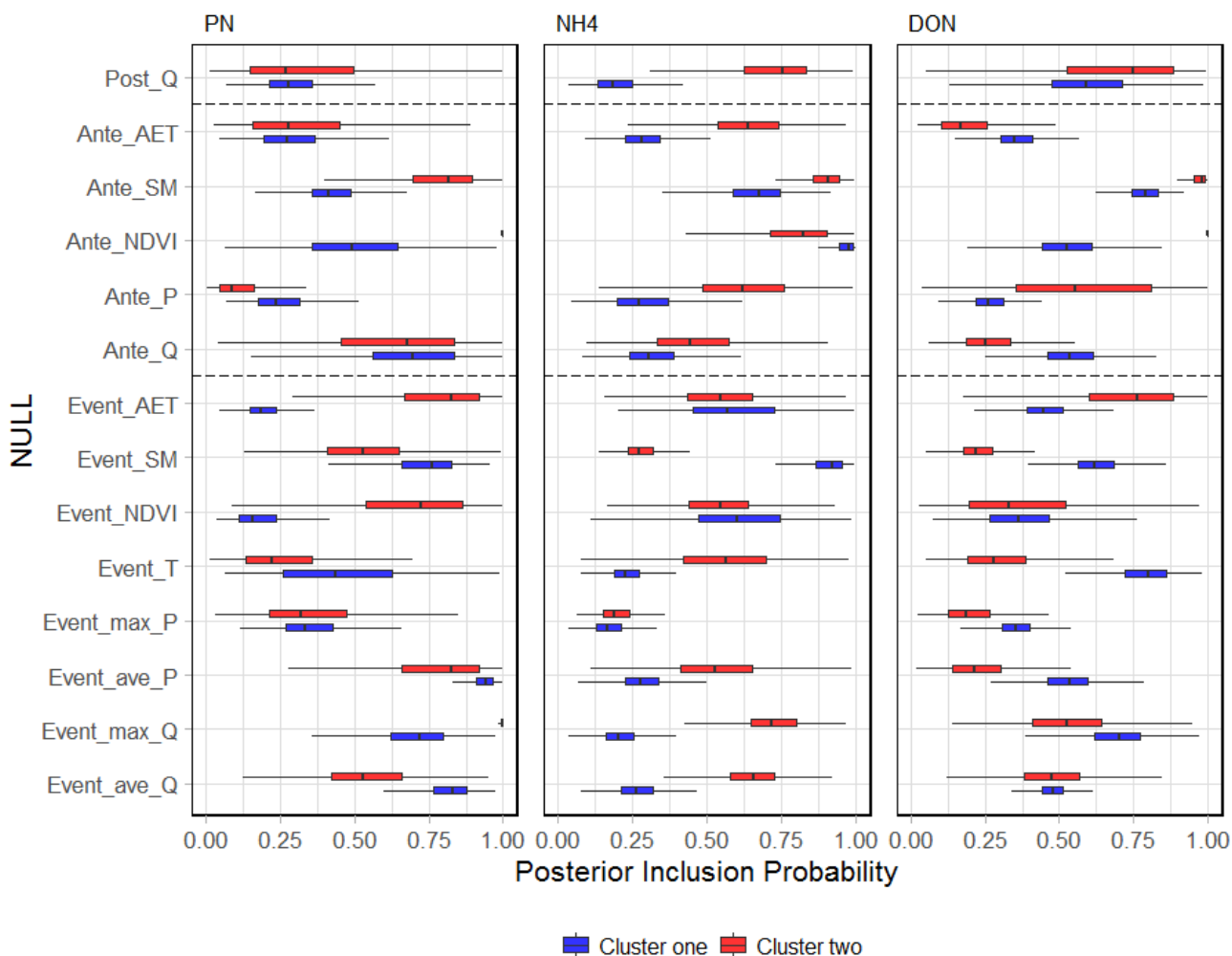
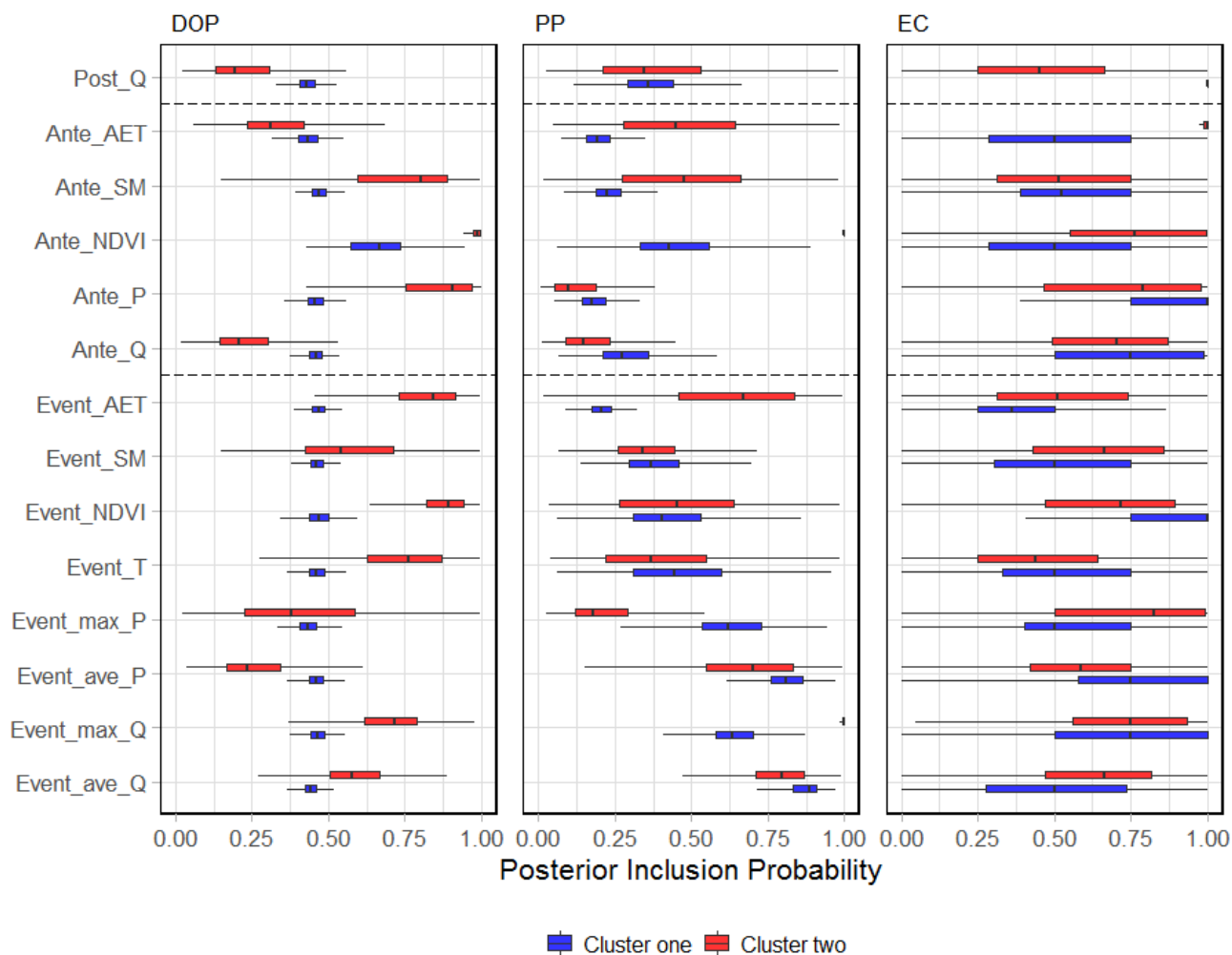


Figure B6: The comparisons of distribution of posterior inclusion probability of individual predictors derived from 1,000 subsampled BMA runs. The interpretation of boxplot is the same as Figure 9. Note: colour represents different clusters: blue - Cluster and red - Cluster two. The definition of abbreviation of each predictor can be found in Table 3.



930

Figure B7: The comparisons of distribution of posterior inclusion probability of individual predictors derived from 1,000 subsampling BMA. The interpretation of boxplot is the same as Figure 3. Note: colour represents different clusters: blue - Cluster one and red - Cluster two.

935

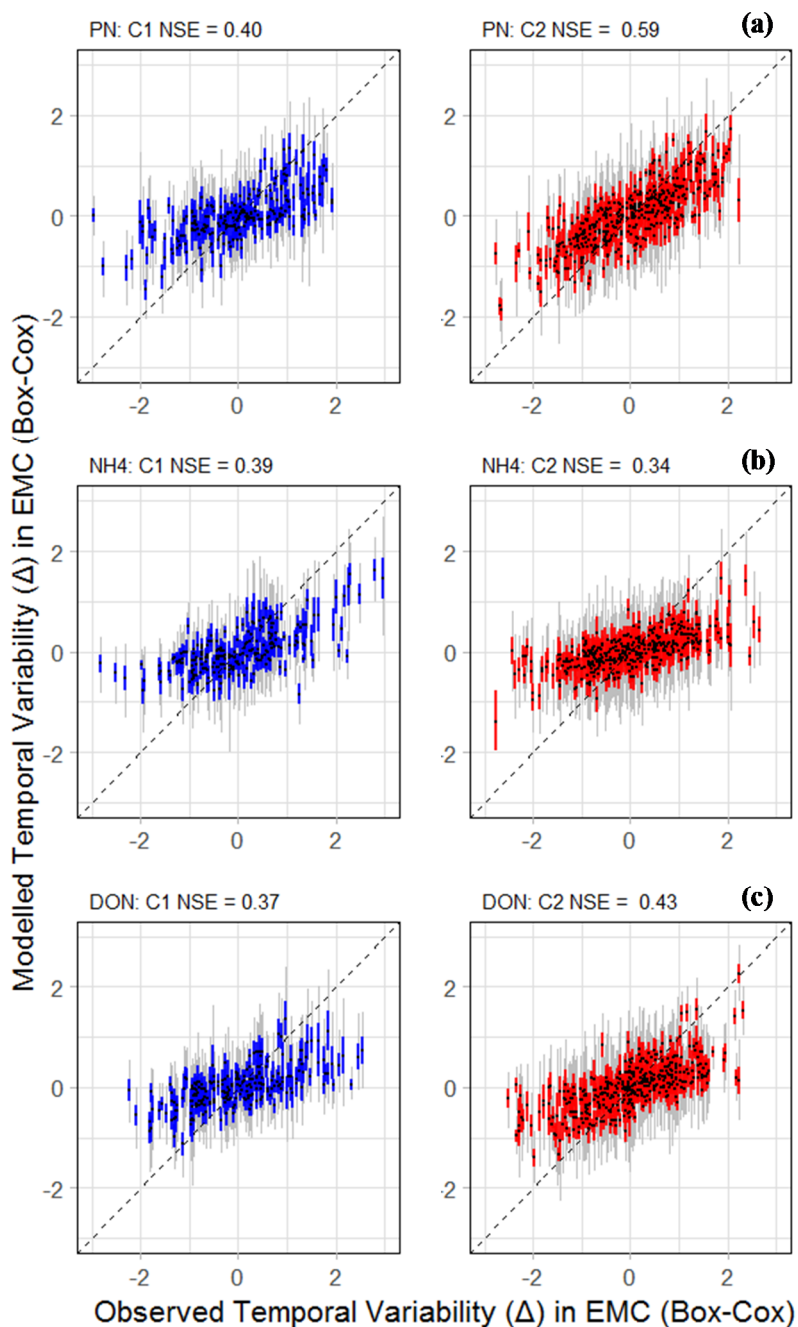
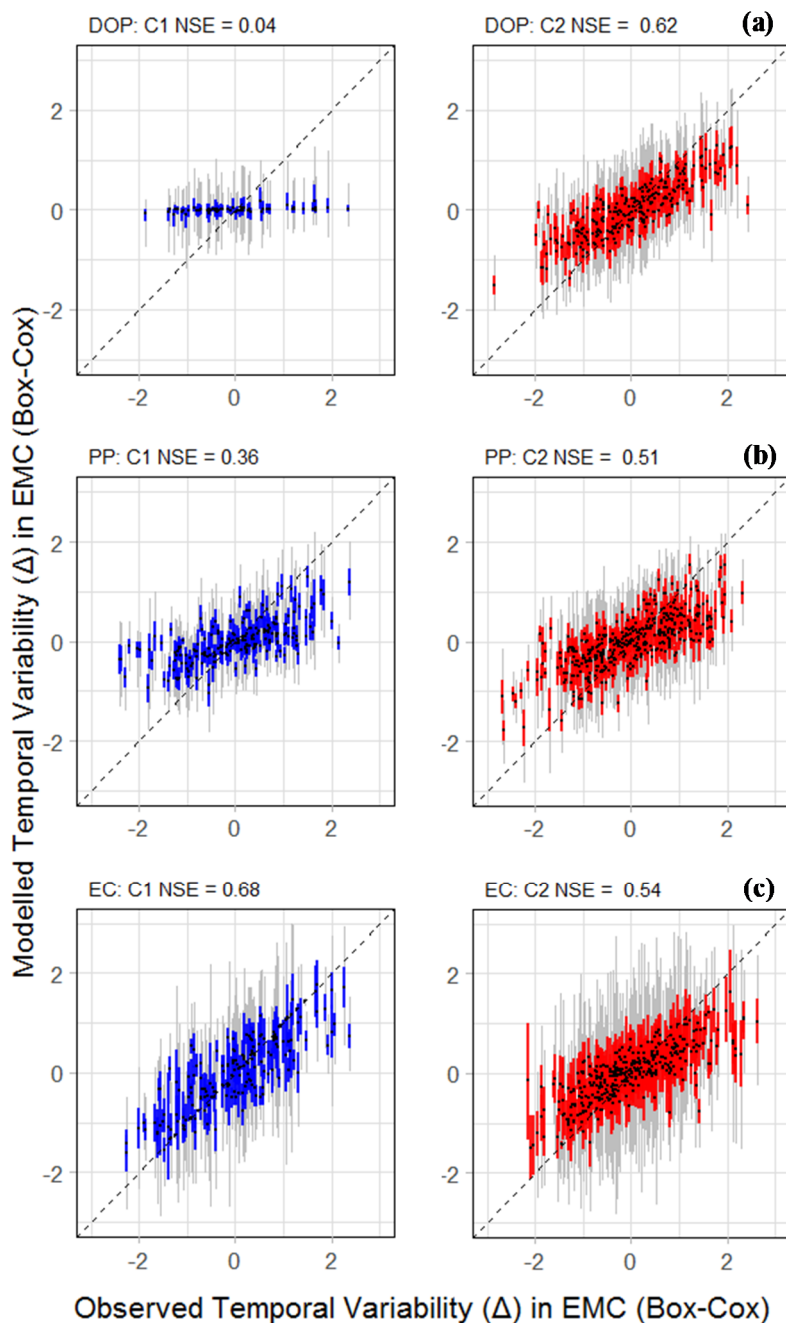


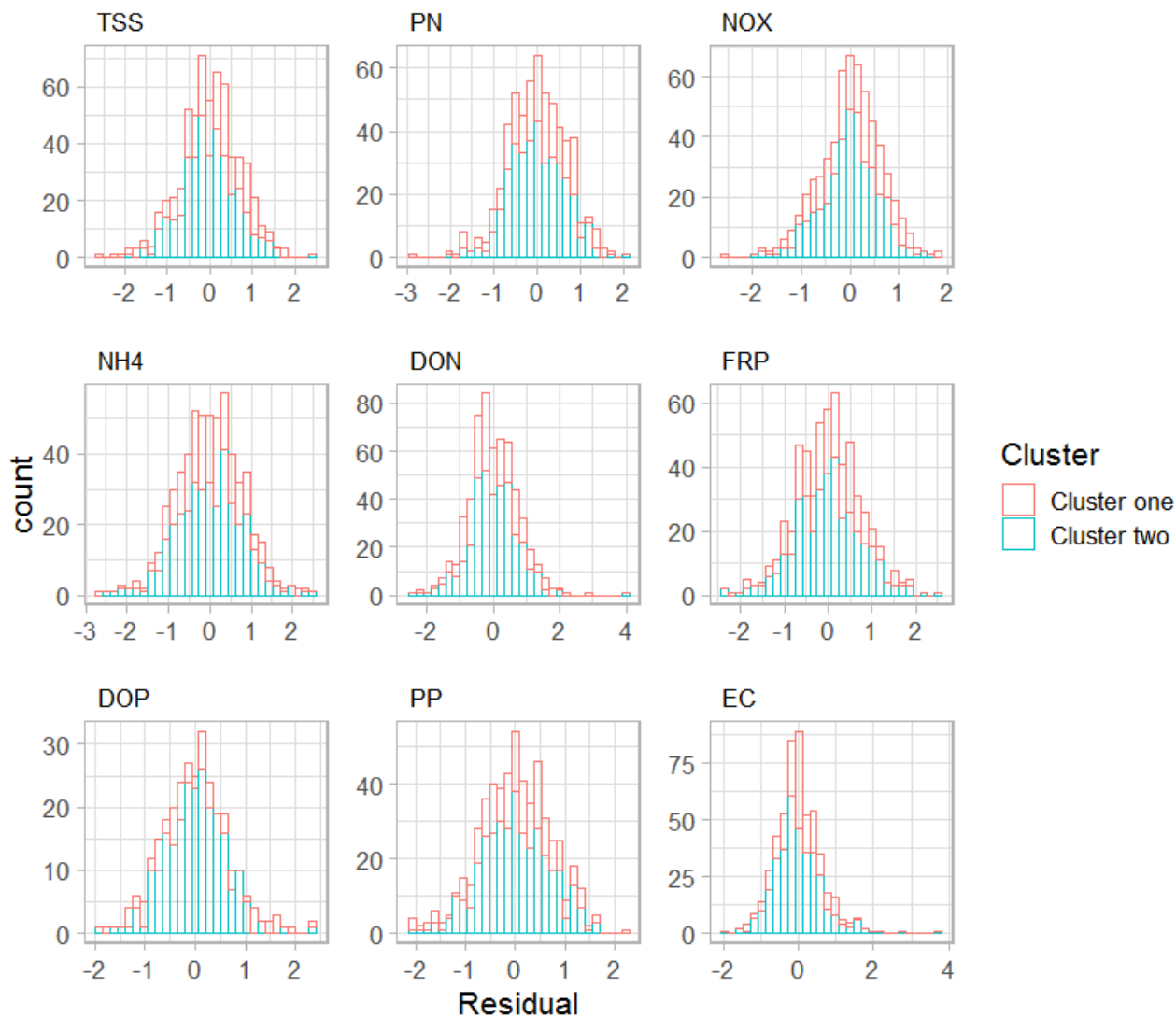
Figure B8: Performance of the BMA models of the temporal variability of nine constituents across 32 sites, represented by prediction intervals from BMA and observed Box-Cox EMC across two clusters of sites for: (a) PN; (b) NH₄ and (c) DON. The NSE values are calculated based on predictions within group- (cluster) level. *Note:* black dots are the prediction median; grey vertical lines are the 95% CI and coloured vertical lines indicates 50% CI: blue - Cluster and red - Cluster two. The dashed black lines is the 1:1 relationship.

940

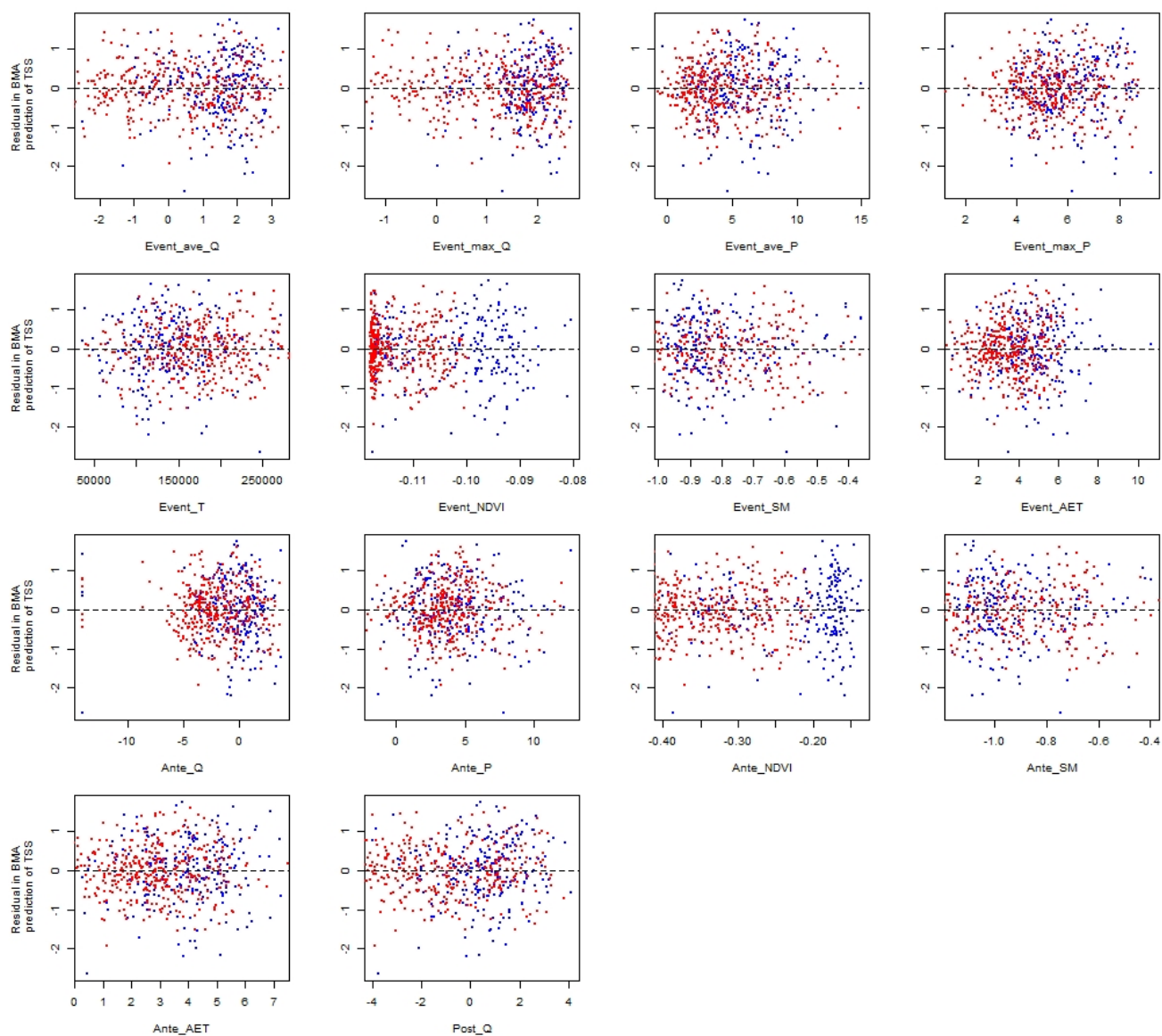


945

Figure B9: Performance of the BMA models of the temporal variability of nine constituents across 32 sites, represented by prediction intervals from BMA and observed Box-Cox EMC across two clusters of sites for: (a) DOP; (b) PP and (c) EC. The NSE values are calculated based on predictions within group- (cluster) level. Note: black dots are the prediction median; grey vertical lines are the 95% CI and coloured vertical lines indicates 50% CI: blue - Cluster and red - Cluster two. The dashed black lines is the 1:1 relationship.



950 **Figure B10: Histograms showing distribution of residuals of nine constituents from BMA predictions. Red – Cluster one; Blue – Cluster two.**



955 **Figure B11: Relationship between residual in median of BMA prediction of TSS and 14 candidate covariates in BMA. Note, difference colours indicate two clusters: Red – Cluster one; Blue – Cluster two.**

960

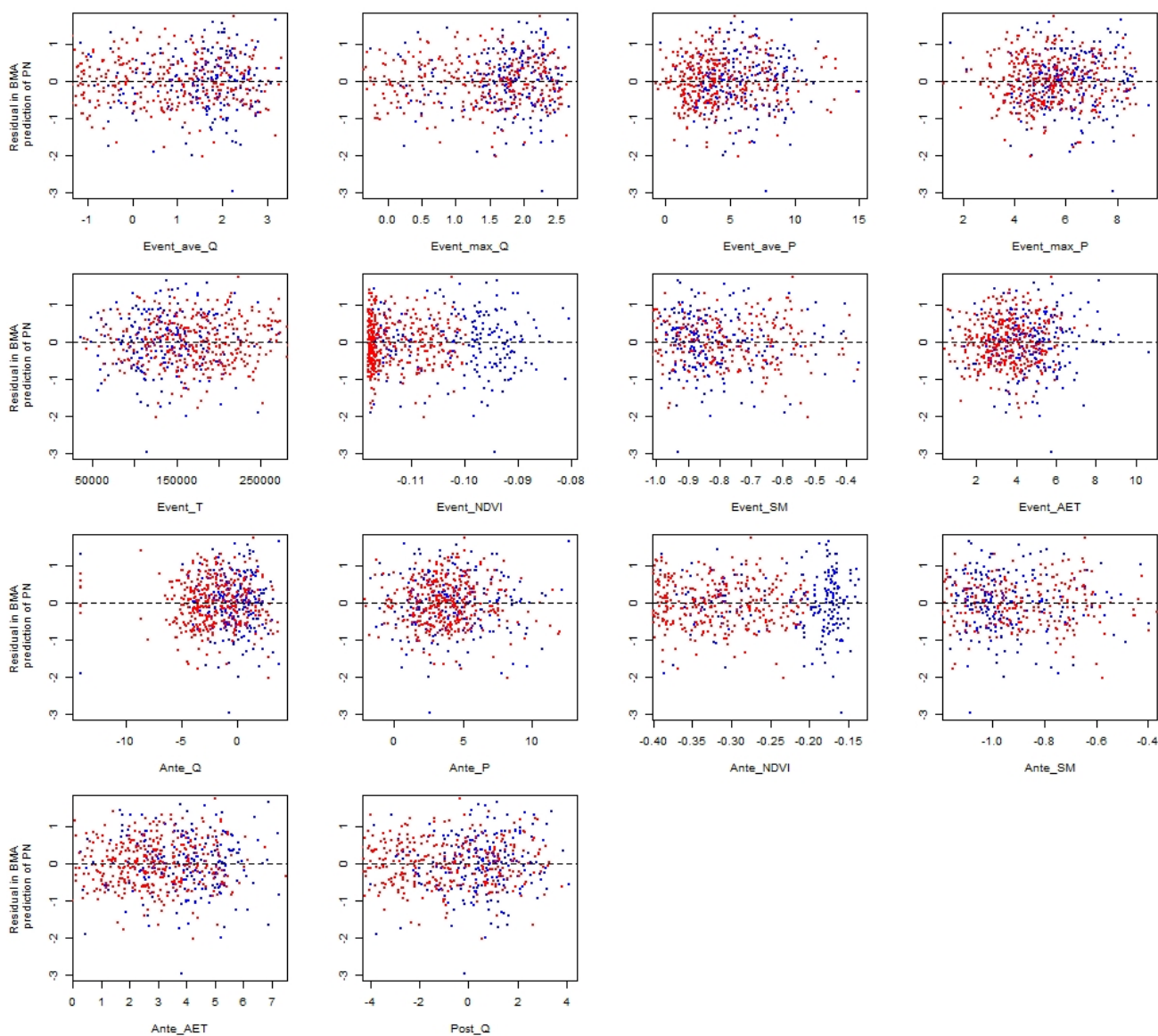
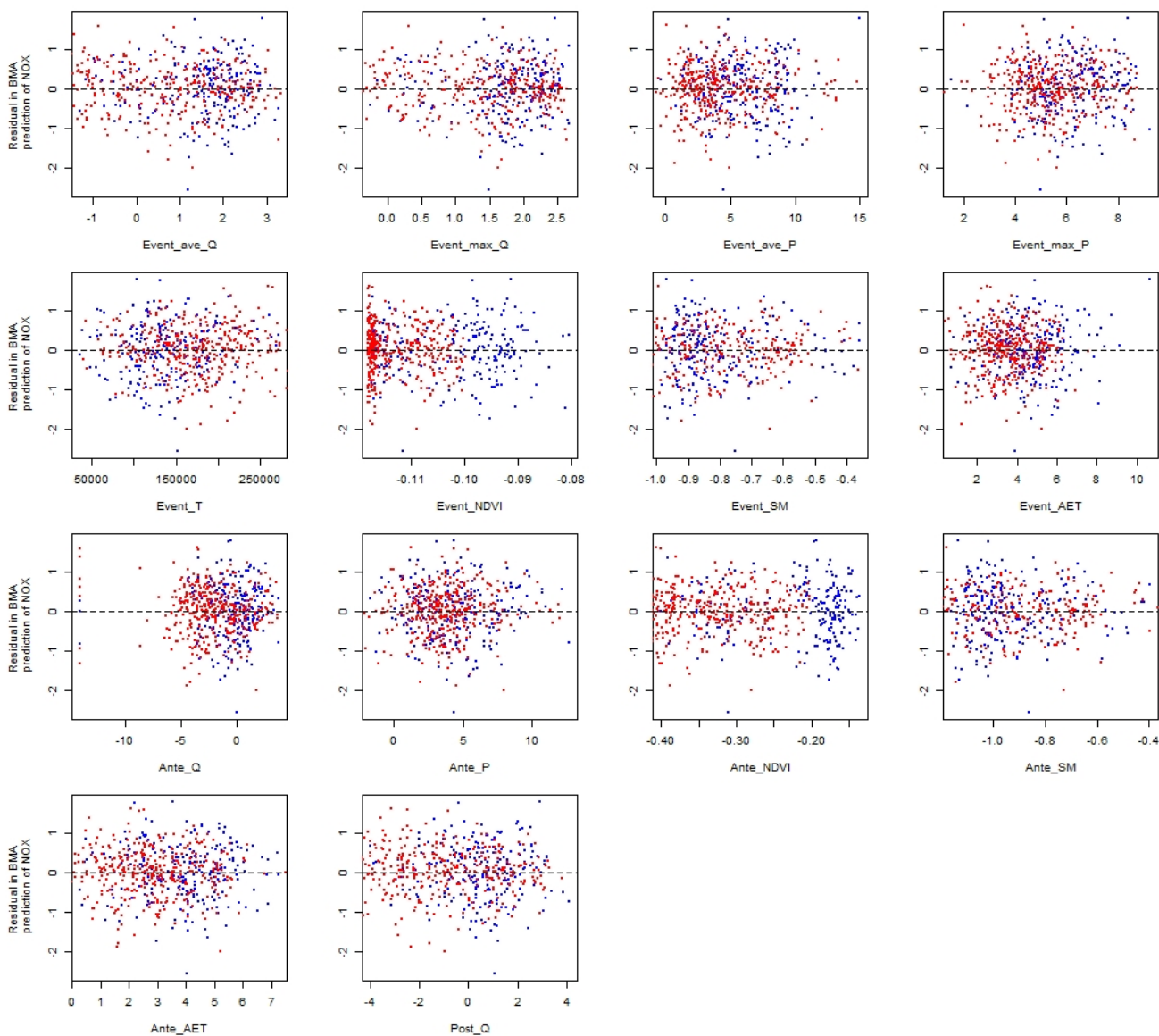


Figure B12: Relationship between residual in median of BMA prediction of PN and 14 candidate covariates in BMA. Note, difference colours indicate two clusters: Red – Cluster one; Blue – Cluster two.



965

Figure B13: Relationship between residual in median of BMA prediction of NO_x and 14 candidate covariates in BMA. Note, difference colours indicate two clusters: Red – Cluster one; Blue – Cluster two.

970

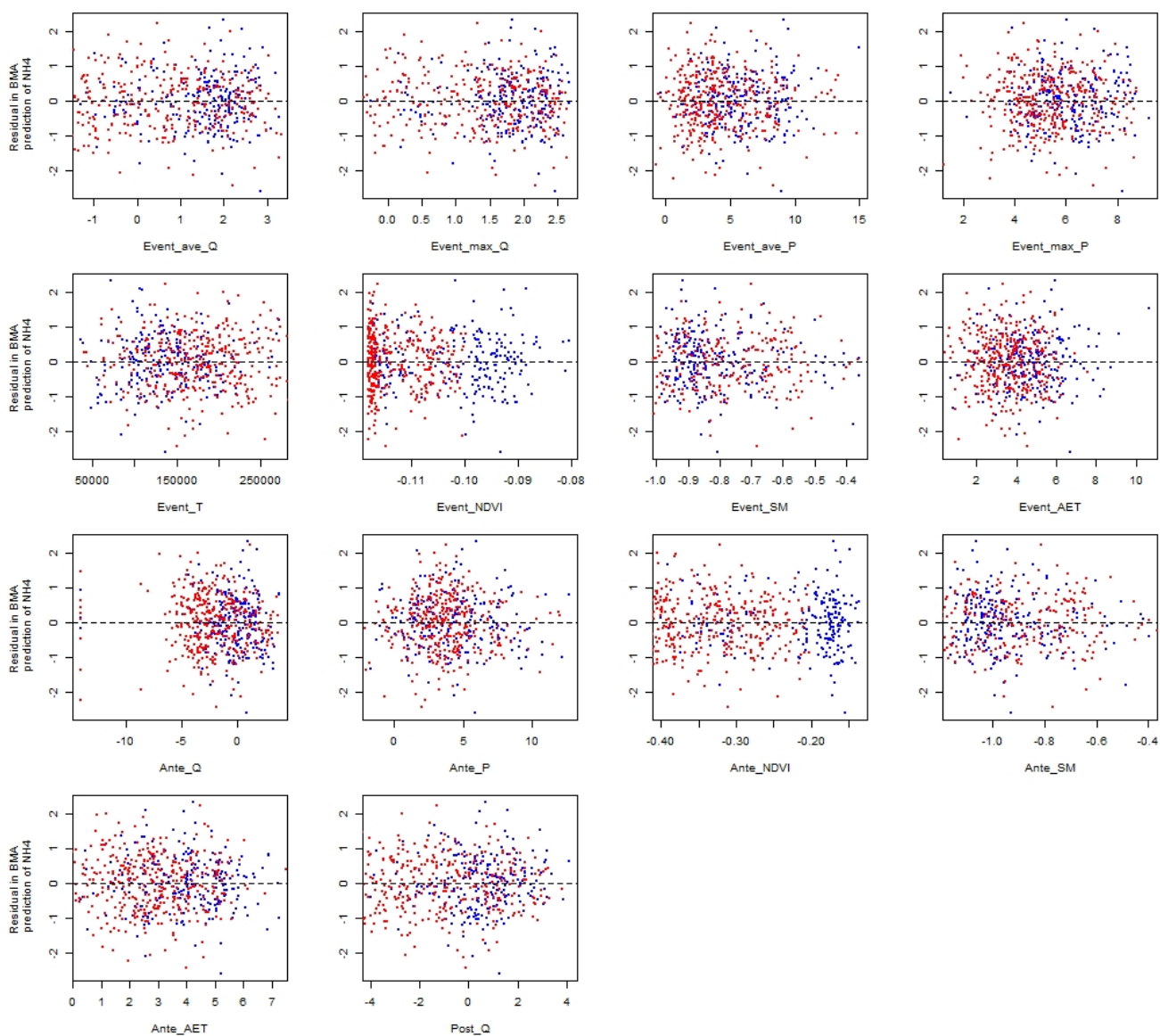


Figure B14: Relationship between residual in median of BMA prediction of NH_4 and 14 candidate covariates in BMA. Note, difference colours indicate two clusters: Red – Cluster one; Blue – Cluster two.

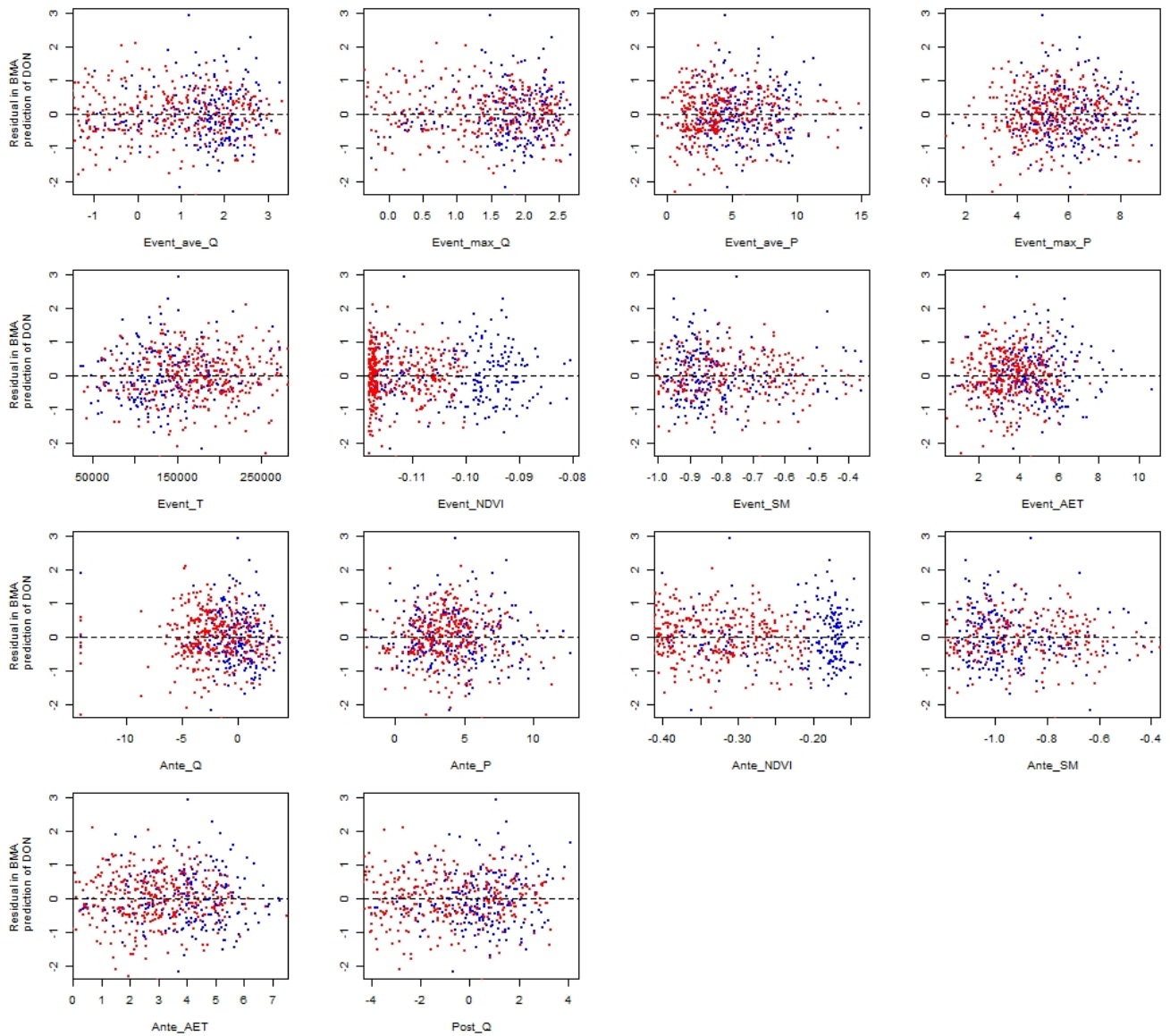
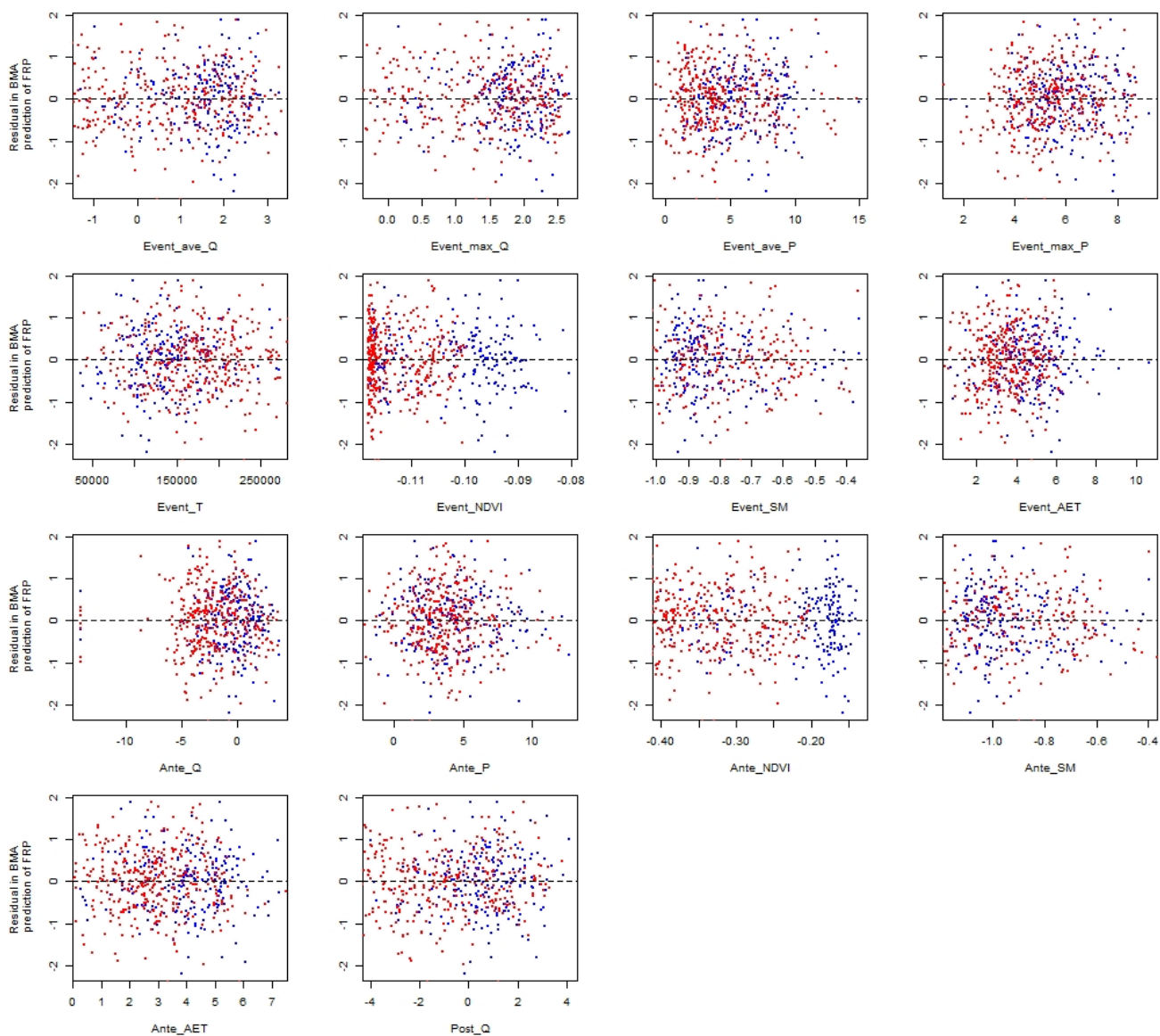
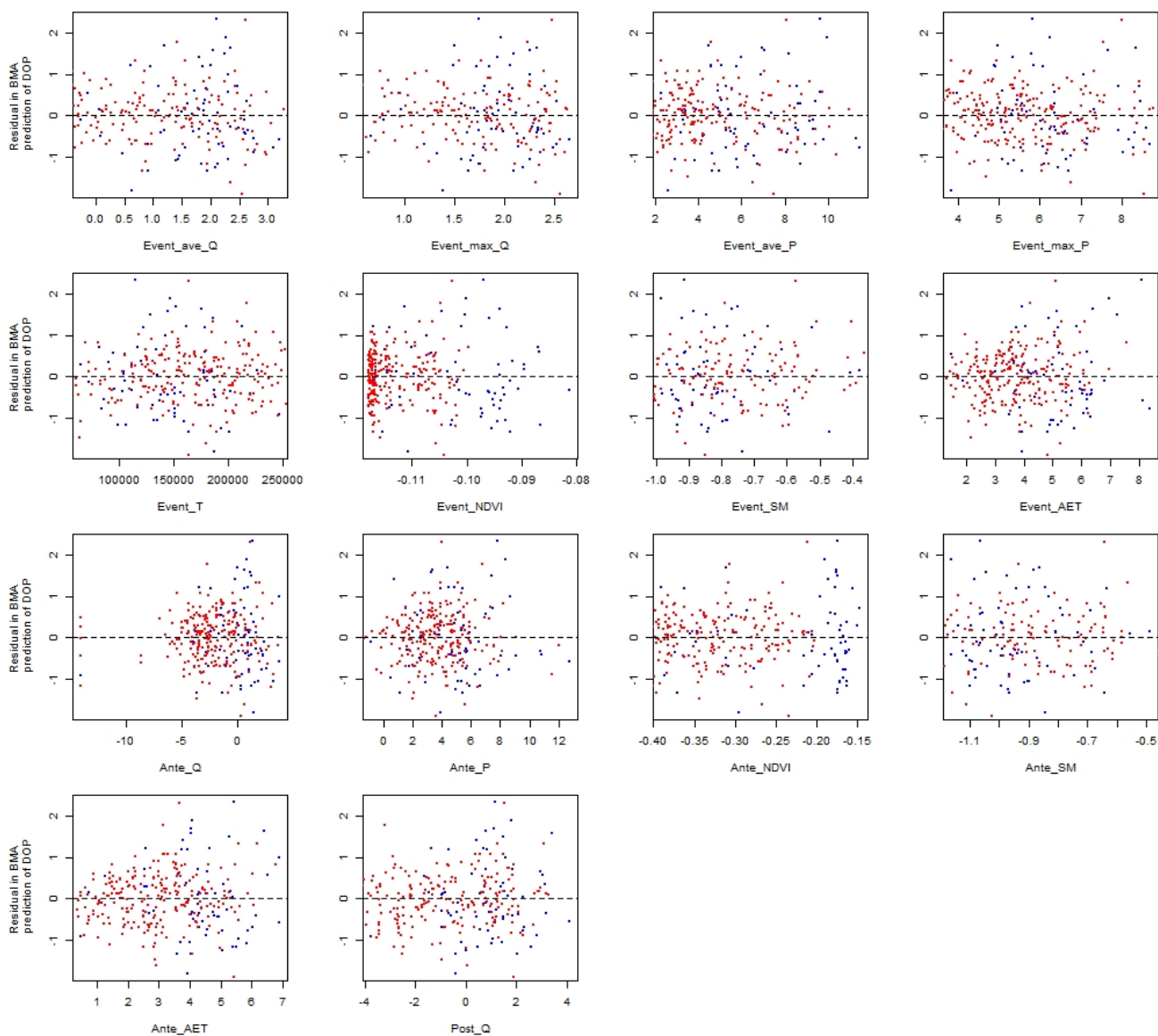


Figure B15: Relationship between residual in median of BMA prediction of DON and 14 candidate covariates in BMA. Note, difference colours indicate two clusters: Red – Cluster one; Blue – Cluster two.

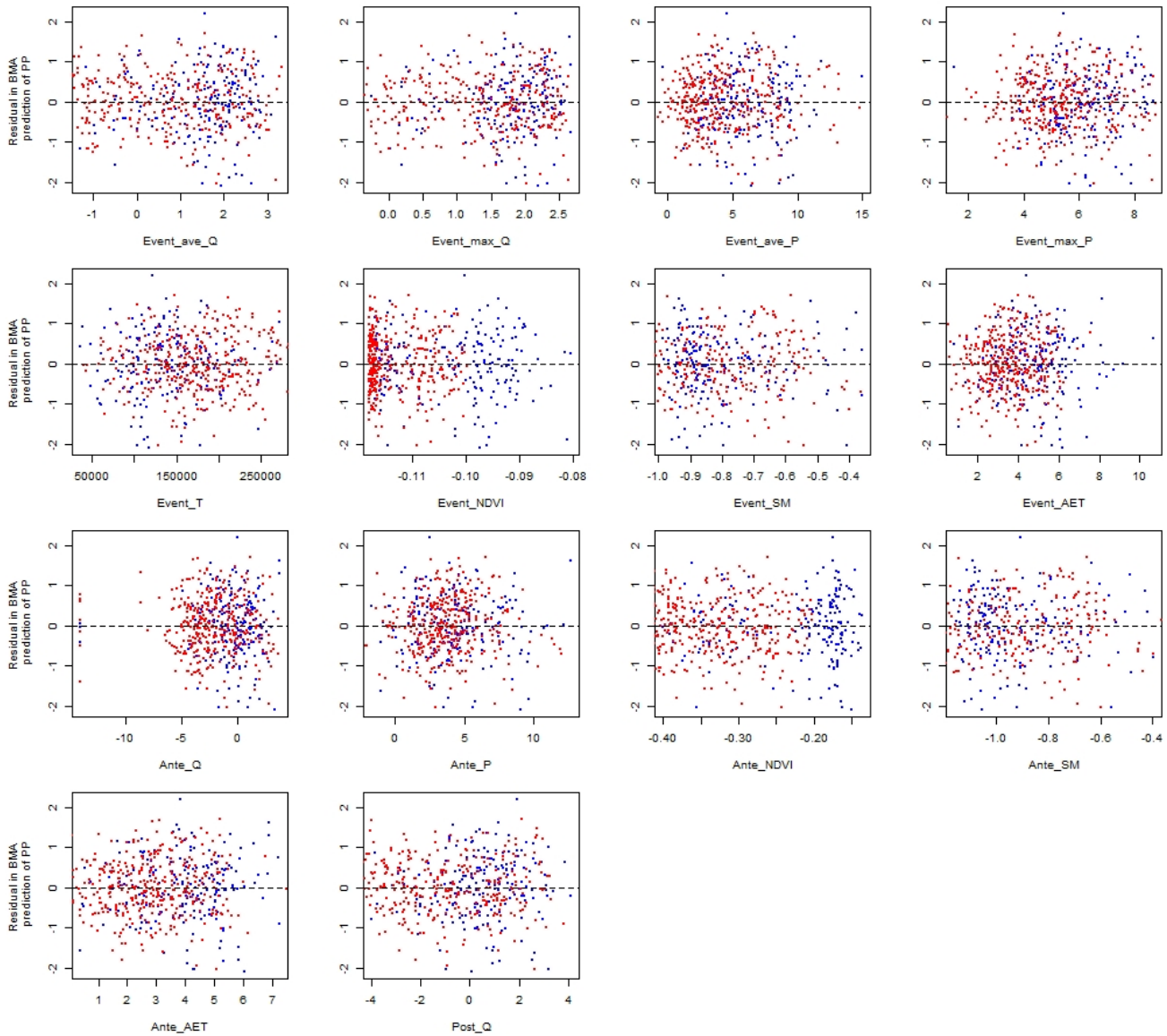


985 **Figure B16:** Relationship between residual in median of BMA prediction of FRP and 14 candidate covariates in BMA. Note, difference colours indicate two clusters: Red – Cluster one; Blue – Cluster two.



990

Figure B17: Relationship between residual in median of BMA prediction of DOP and 14 candidate covariates in BMA. Note, difference colours indicate two clusters: Red – Cluster one; Blue – Cluster two.



995 **Figure B18: Relationship between residual in median of BMA prediction of PP and 14 candidate covariates in BMA. Note, difference colours indicate two clusters: Red – Cluster one; Blue – Cluster two.**

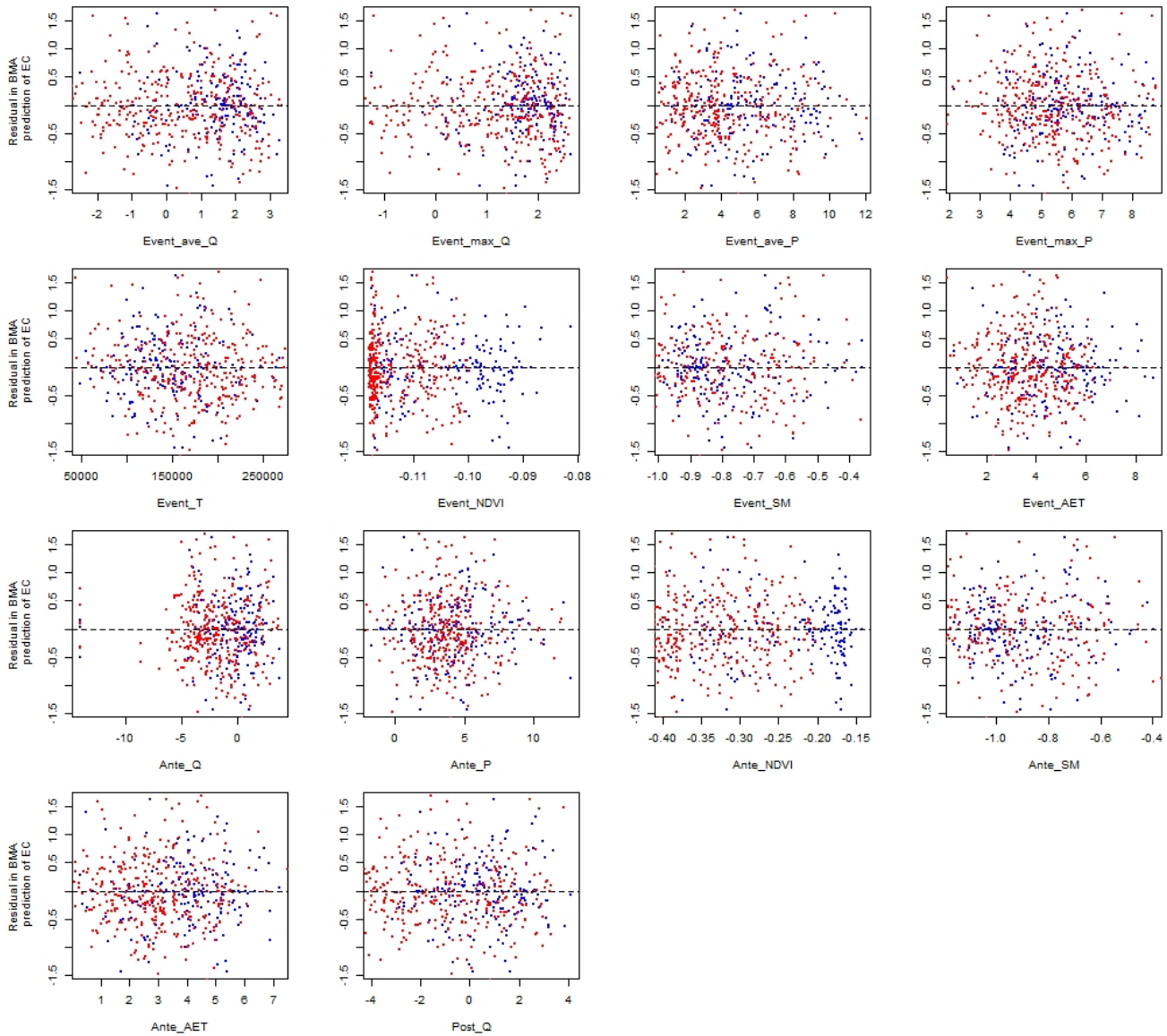


Figure B19: Relationship between residual in median of BMA prediction of EC and 14 candidate covariates in BMA. Note, difference colours indicate two clusters: Red – Cluster one; Blue – Cluster two.



Appendix C - Table

1010 **Table C1. Description of 32 sites in the GBR catchments**

NRM	Site ID	River and site name	Latitude/°	Longitude/°	Catchment area / km ²
Cape York	105107A	Normanby River at Kalpowar Crossing	-14.9185	144.2100	12934
Wet tropics	110001D	Barron River at Myola	-16.7998	145.6121	1945
Wet tropics	110002A	Barron River at Mareeba	-17.0022	145.4293	836
Wet tropics	110003A	Barron River at Picnic Crossing	-17.2591	145.5386	228
Wet tropics	1110056	Mulgrave River at Deeral	-17.2075	145.9264	785
Wet tropics	1111019	Russell River at East Russell	-17.2672	145.9544	524
Wet tropics	1120049	North Johnstone River at Old Bruce Hwy Bridge (Goondi)	-17.5059	145.9920	959
Wet tropics	112004A	North Johnstone River at Tung Oil	-17.5456	145.9325	925
Wet tropics	112101B	South Johnstone River at Upstream Central Mill	-17.6106	145.9789	400
Wet tropics	113006A	Tully River at Euramo	-17.9936	145.9411	1450
Wet tropics	113015A	Tully River at Tully Gorge National Park	-17.7727	145.6507	482
Wet tropics	116001F	Herbert River at Ingham	-18.6328	146.1427	8581
Burdekin	119101A	Barratta Creek at Northcote	-19.6923	147.1688	753
Burdekin	120001A	Burdekin River at Home Hill	-19.6436	147.3958	129939
Burdekin	120002C	Burdekin River at Sellheim	-20.0078	146.4369	36290
Burdekin	120301B	Belyando River at Gregory Development Rd.	-21.5423	146.8656	35410
Burdekin	120302B	Cape River at Taemas	-20.9996	146.4271	16070
Burdekin	120310A	Suttor River at Bowen Developmental Road	-21.5375	147.0424	10760
Mackay Whitsunday	124001B	O'Connell River at Stafford's Crossing	-20.6526	148.5730	342
Mackay Whitsunday	1240062	O'Connell River at Caravan Park	-20.5664	148.6117	825
Mackay Whitsunday	125013A	Pioneer River at Dumbleton Pump Station	-21.1441	149.0753	1485
Mackay Whitsunday	126001A	Sandy Creek at Homebush	-21.2831	149.0228	326
Fitzroy	1300000	Fitzroy River at Rockhampton	-23.3175	150.4819	139159
Fitzroy	130206A	Theresa Creek at Gregory Highway	-23.4292	148.1514	8485
Fitzroy	130302A	Dawson River at Taroom	-25.6376	149.7901	15850
Fitzroy	130504B	Comet River at Comet Weir	-23.6125	148.5514	16460
Burnett Mary	136002D	Burnett River at Mt Lawless	-25.5447	151.6549	29360
Burnett Mary	136004A	Jones Weir HW	-25.5948	151.2964	21700
Burnett Mary	136014A	Burnett River at Ben Anderson Barrage Head Water	-24.8896	152.2922	32891
Burnett Mary	136094A	Burnett River at Jones Weir (TW)	-25.5948	151.2974	21700



Burnett Mary	136106A	Burnett River at Eidsvold	-25.4023	151.1033	7117
Burnett Mary	138014A	Mary River at Home Park	-25.7683	152.5274	6845

Table C2. Number of EMCs for each constituent

Cluster	TSS	PN	NO _x	NH ₄	DON	FRP	DOP	PP	EC
One	225	207	218	217	215	210	66	186	174
Two	381	370	372	370	373	372	231	366	354
% of event monitored	43	41	42	42	42	41	21	39	37

1015

Table C3. Posterior inclusion probability of individual predictor derived from BMA on two clusters of sites.

Predictor	TSS		PN		NO _x		NH ₄		DON		FRP		DOP		PP		EC	
	Cluster one	Cluster two	Cluster one	Cluster two	Cluster one	Cluster two	Cluster one	Cluster two	Cluster one	Cluster two	Cluster one	Cluster two	Cluster one	Cluster two	Cluster one	Cluster two	Cluster one	Cluster two
Event_ave_Q	<i>0.93</i>	<i>0.47</i>	<i>0.87</i>	<i>0.49</i>	<i>0.97</i>	<i>0.56</i>	0.21	0.68	0.47	0.47	0.33	0.38	0.46	0.58	<i>0.92</i>	<i>0.85</i>	<i>1.00</i>	<i>0.86</i>
Event_max_Q	0.73	<i>1.00</i>	0.76	<i>1.00</i>	0.33	0.58	0.14	0.79	0.79	0.60	<i>0.94</i>	0.43	0.46	<i>0.85</i>	0.66	<i>0.99</i>	<i>1.00</i>	0.63
Event_ave_P	<i>0.92</i>	<i>0.92</i>	<i>0.98</i>	<i>0.92</i>	0.32	0.07	0.25	0.51	0.52	0.16	0.79	<i>0.96</i>	0.45	0.24	<i>0.86</i>	<i>0.82</i>	0.67	<i>0.90</i>
Event_max_P	0.24	0.48	0.24	0.29	0.47	0.01	0.10	0.13	0.31	0.17	0.68	0.44	0.41	0.27	0.67	0.15	<i>1.00</i>	<i>0.96</i>
Event_T	0.07	0.27	0.50	0.21	0.19	<i>0.98</i>	0.16	0.58	<i>0.88</i>	0.26	<i>0.86</i>	<i>0.90</i>	0.48	0.78	0.53	0.61	<i>1.00</i>	0.64
Event_ND_VI	0.03	0.27	0.09	<i>0.89</i>	0.77	0.55	0.68	0.62	0.35	0.34	0.38	0.49	0.46	0.97	0.39	0.52	0.75	0.79
Event_SM	0.54	0.21	<i>0.83</i>	0.58	<i>0.99</i>	0.38	<i>0.96</i>	0.21	0.64	0.19	0.59	0.48	0.47	0.66	0.40	0.35	0.33	0.60
Event_AET	0.13	0.07	0.12	<i>0.90</i>	0.61	<i>1.00</i>	0.68	0.57	0.43	<i>0.86</i>	0.57	0.38	0.51	0.87	0.17	<i>0.81</i>	0.33	0.10
Ante_Q	0.23	0.18	0.76	0.76	0.15	<i>0.98</i>	0.30	0.37	0.56	0.25	0.36	<i>0.86</i>	0.47	0.17	0.25	0.12	0.33	0.59
Ante_P	0.20	0.05	0.22	0.06	0.16	0.03	0.25	0.70	0.22	0.75	0.25	<i>0.88</i>	0.44	0.98	0.13	0.06	<i>0.81</i>	<i>0.91</i>
Ante_NDVI	0.23	<i>1.00</i>	0.56	<i>1.00</i>	<i>0.86</i>	<i>1.00</i>	<i>0.99</i>	<i>0.89</i>	0.47	<i>1.00</i>	<i>0.97</i>	<i>0.93</i>	0.67	<i>1.00</i>	0.44	<i>1.00</i>	0.33	0.61
Ante_SM	0.13	0.74	0.38	<i>0.90</i>	0.79	<i>1.00</i>	0.63	<i>0.96</i>	<i>0.83</i>	<i>0.99</i>	<i>0.90</i>	<i>0.95</i>	0.50	<i>0.89</i>	0.19	0.59	<i>1.00</i>	0.70
Ante_AET	0.09	<i>0.81</i>	0.27	0.31	0.31	0.60	0.20	0.72	0.33	0.10	0.42	0.48	0.42	0.30	0.14	0.61	0.33	<i>1.00</i>
Post_Q	0.41	0.07	0.21	0.27	0.18	<i>1.00</i>	0.16	0.77	0.66	<i>0.80</i>	0.17	<i>0.81</i>	0.42	0.10	0.32	0.37	<i>1.00</i>	0.63

Note: Posterior inclusion probability ≥ 0.8 in italic.